BIOCHEMISTRY

10.1126/sciadv.1500968

A novel persulfide detection method reveals protein persulfide- and polysulfide-reducing functions of thioredoxin and glutathione systems

Éva Dóka,[1] Irina Pader,[2] Adrienn Bíró,[1] Katarina Johansson,[2] Qing Cheng,[2] Krisztina Ballagó,[1] Justin R. Prigge,[3] Daniel Pastor-Flores,[4] Tobias P. Dick,[4] Edward E. Schmidt,[3] Elias S. J. Arnér,[2] Péter Nagy[1]*

Hydrogen sulfide signaling involves persulfide formation at specific protein Cys residues. However, overcoming current methodological challenges in persulfide detection and elucidation of Cys regeneration mechanisms from persulfides are prerequisites for constructing a bona fide signaling model. We here establish a novel, highly specific protein persulfide detection protocol, ProPerDP, with which we quantify 1.52 ± 0.6 and 11.6 ± 6.9 μg/mg protein steady-state protein persulfide concentrations in human embryonic kidney 293 (HEK293) cells and mouse liver, respectively. Upon treatment with polysulfides, HEK293 and A549 cells exhibited increased protein persulfidation. Deletion of the sulfide-producing cystathionine-γ-lyase or cystathionine-β-synthase enzymes in yeast diminished protein persulfide levels, thereby corroborating their involvement in protein persulfidation processes. We here establish that thioredoxin (Trx) and glutathione (GSH) systems can independently catalyze reductions of inorganic polysulfides and protein persulfides. Increased endogenous persulfide levels and protein persulfidation following polysulfide treatment in thioredoxin reductase-1 (TrxR1) or thioredoxin-related protein of 14 kDa (TRP14) knockdown HEK293 cells indicated that these enzymes constitute a potent regeneration system of Cys residues from persulfides in a cellular context. Furthermore, TrxR1-deficient cells were less viable upon treatment with toxic amounts of polysulfides compared to control cells. Emphasizing the dominant role of cytosolic disulfide reduction systems in maintaining sulfane sulfur homeostasis in vivo, protein persulfide levels were markedly elevated in mouse livers where hepatocytes lack both TrxR1 and glutathione reductase (TR/GR-null). The different persulfide patterns observed in wild-type, GR-null, and TR/GR-null livers suggest distinct roles for the Trx and GSH systems in regulating subsets of protein persulfides and thereby fine-tuning sulfide signaling pathways.

INTRODUCTION

Since the neuromodulator function of hydrogen sulfide (H_2S) was discovered about 20 years ago (*1*), extensive research has revealed master regulator properties of H_2S in a wide array of physiological processes in almost all forms of life (*2*). In addition to being vital for normal human physiology, H_2S also plays central roles in many pathophysiological events, substantiating sulfide-mediated signaling as a drug target (*3*, *4*). However, the understanding of the molecular mechanisms for H_2S signaling remains very limited (*5*). Enzyme and protein regulation via persulfidation, that is, formation of persulfide (-SSH) moieties (a process also known as protein S-sulfhydration), at regulatory cysteine (Cys) residues is widely suggested as a major pathway (*5*, *6*). Furthermore, sulfane sulfur species (a collective name for compounds containing forms of sulfide with an oxidation state of 0) are now recognized as mediators in redox biology (*7*, *8*) and nitric oxide signaling (*9*–*12*). Thus, increasing attention in the field of redox signaling and sulfur biology has been diverted to the biological roles of inorganic polysulfides (HS_x^-) (*13*) and protein persulfides (*7*, *14*).

Despite a rapid evolution of fluorescent probes (*15*) and several protein persulfide detection methods (*16*), there remains a very limited understanding of the role of sulfane sulfur species in signaling pathways and cellular redox homeostasis (*17*). For example, recently reported relatively high cellular persulfide levels of up to 0.1 mM (*7*) were argued to be in contrast with the notion of a highly reducing environment in the cytosol that would counteract their formation (*18*), thus highlighting the need of optimized and more specific persulfide detection methods. In this context, it should also be noted that although persulfide formation pathways have been rather extensively studied, the reducing mechanisms that can regenerate native forms of Cys residues from persulfide species remain largely elusive. Two recent reports have suggested the involvement of thioredoxin (Trx) in metabolism of Cys persulfides (*19*, *20*), but there remains a lack of thorough mechanistic studies of such activities.

Here, we report the development and validation of a novel, easy-to-use, and highly specific Protein Persulfide Detection Protocol (ProPerDP), which can be used with intact cells and tissue samples. We report the capacities of thioredoxin reductase-1 (TrxR1), Trx1, and the alternative TrxR1-dependent redox active thioredoxin-related protein of 14 kDa (TRP14) (*21*) to reduce polysulfides and protein persulfide species and, utilizing ProPerDP, we demonstrate their impacts on cellular protein persulfide levels. Apart from its recently recognized nitrosothiol- and cystine-reducing properties (*22*), our results reveal that TRP14 is highly efficient in catalyzing protein persulfide and HS_x^- reduction. In addition, our results indicate that cells with a compromised Trx system exhibit decreased viability in the presence of toxic amounts of inorganic polysulfides. Furthermore, we show that the glutaredoxin (Grx)/glutathione reductase (GR)/glutathione (GSH) machinery can also catalytically reduce polysulfides and protein persulfides. Finally, using ProPerDP on mouse liver samples lacking GR and/or TrxR1

[1]Department of Molecular Immunology and Toxicology, National Institute of Oncology, Ráth György utca 7-9, Budapest 1122, Hungary. [2]Division of Biochemistry, Department of Medical Biochemistry and Biophysics, Karolinska Institutet, SE-171 77 Stockholm, Sweden. [3]Department of Microbiology and Immunology, Montana State University, Cooley Hall, PO Box 173520, Bozeman, MT 59717, USA. [4]Division of Redox Regulation, German Cancer Research Center (DKFZ), DKFZ-ZMBH Alliance, Im Neuenheimer Feld 280, 69120 Heidelberg, Germany.
*Corresponding author. E-mail: peter.nagy@oncol.hu

in hepatocytes, we demonstrate the physiological significance of the Trx and GSH systems to maintain sulfane sulfur homeostasis and suggest their involvement in sulfide signaling.

RESULTS

ProPerDP: A novel protein persulfide detection protocol

We here developed an easy, convenient, and reliable protein persulfide detection protocol (ProPerDP), which we found to yield high specificity (Fig. 1). In the initial step, protein Cys thiol (-SH) and persulfide (-SSH) functional groups are alkylated using the biotin-labeled alkylating agent EZ-Link Iodoacetyl-PEG$_2$-Biotin (IAB) (Fig. 1, Sample 1) and can thereafter be pulled down from a protein mixture using streptavidin-coated magnetic beads. Other oxidized Cys derivatives, such as disulfides, are not alkylated under the conditions of ProPerDP and remain in the supernatant (Fig. 1, Sample 2). Cys sulfenic acids (-SOH) or nitrosothiols (-SNO) may become alkylated to some extent, but such reactions would generate thioethers (-SR) just as with the free thiols and hence will not appear as false positives in the final persulfide fraction (Sample 3). Derivatized persulfides are separated from the original thiol groups in a reduction step, where the thioethers (the thiol alkylation products) will remain bound to the beads. However, the dialkyl disulfides derived from the protein persulfides that were present in the original sample are selectively cleaved off and can thus be quantified and subsequently visualized on SDS–polyacrylamide gel electrophoresis (SDS-PAGE) (Fig. 1, Sample 3). The thioether-containing proteins can also be detected by SDS-PAGE upon their release from the beads by boiling in SDS-containing sample buffer (Fig. 1, Sample 4).

Persulfide formation on human serum albumin

Human serum albumin (HSA) contains a single, freely accessible Cys residue (Cys^{34}) that can provide a site of protein persulfidation and was used as a model protein to validate the ProPerDP method. HSA persulfide (HSA-SSH) was generated by reacting HSA with HS_x^-. HSA-SSH formation was confirmed by our previously reported indirect measurement of protein-associated sulfane sulfur in concentrated solutions of purified protein samples (*23*). This protocol is based on the quantification of sulfide that is liberated upon reduction of desalted protein persulfide samples by a modified monobromobimane method (*24*). 10.2 ± 1.4 μM H_2S (mean ± SD from n = 5 experiments) was liberated from 10 μM purified, polysulfide-treated HSA, suggesting that most of the free Cys^{34} can be persulfidated/polysulfidated by excess HS_x^-. With these HSA-SSH samples, we validated that ProPerDP indeed detects protein persulfides in a specific manner, with no background signal seen if the persulfides were reduced before alkylation {S3 lanes in the ±TCEP [tris(2-carboxyethyl)phosphine] samples in Fig. 2A}. A decline in persulfide content was observed upon incubation of HSA-SSH in the presence of added sulfide before the alkylation step in a dose-dependent manner (Fig. 2A′ and fig. S1), confirming our previous observation that persulfidation is an equilibrium process that can be shifted by the addition of either product or reactant species (*25*). However, depending on the nature of the persulfidated Cys residues, such equilibrium (reaction 1) can be largely shifted either to the left, as is the case with phosphatase and tensin homolog (PTEN) (*23*), or to the right, as with TNB (2-nitro-5-thiobenzoic acid) that was derived from DTNB [5,5′-dithiobis-(2-nitrobenzoic acid)] (*25*).

$$\mathrm{RSSH} + \mathrm{H_2S} \rightleftharpoons \mathrm{RSH} + \mathrm{HSSH} \quad (1)$$

Using Coomassie staining and Western blot analyses, ProPerDP also allowed visualization of HSA-SSH formation in HS_x^--treated plasma samples in a concentration-dependent manner (Fig. 2, B and C). Endogenous HSA-SSH was not detectable, and in contrast to previous suggestions (*26*, *27*), sulfide treatment of plasma samples could not generate substantial amounts of HSA-SSH in our hands (Fig. 2C′). Although HSA

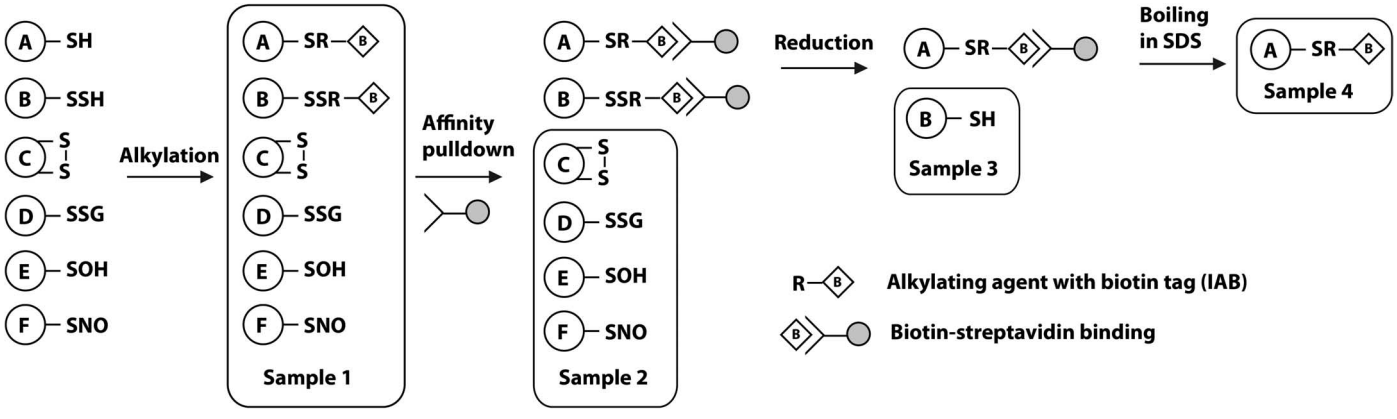

Fig. 1. Protein Persulfide Detection Protocol. Thiol and persulfide functional groups are alkylated by IAB to form the corresponding thioether and dialkyl disulfide derivatives, respectively (-R denotes the electrophile moiety of the alkylating agent). Oxidized Cys residues of proteins in the original sample (Sample 1) will not be derivatized by IAB. Affinity purification of alkylated proteins is achieved by pulldown with streptavidin-coated magnetic beads, leaving proteins only containing oxidized Cys residues in the supernatant (Sample 2). Resuspension of purified beads in a reducing buffer selectively cleaves the original persulfides off as thiols, which can be analyzed after separation with recovery from the beads, thus allowing the determination of protein persulfides (Sample 3). Note that some sulfenic acid (-SOH) or nitrosothiol (-SNO) derivatives might become alkylated in Sample 1, but these reactions give thioethers such as free thiols and hence do not appear as false positives in Sample 3. Native Cys residues with free thiols in the original sample will not be released from the beads by reduction but can be recovered by boiling of the beads in SDS (Sample 4). The diamond symbol (◊) denotes the biotin tag, and the pictogram in the inset refers to the biotin-streptavidin binding interaction. The order and nomenclature of the samples are maintained for all gels and blots in this study, thereby referred to as S1 to S4, respectively.

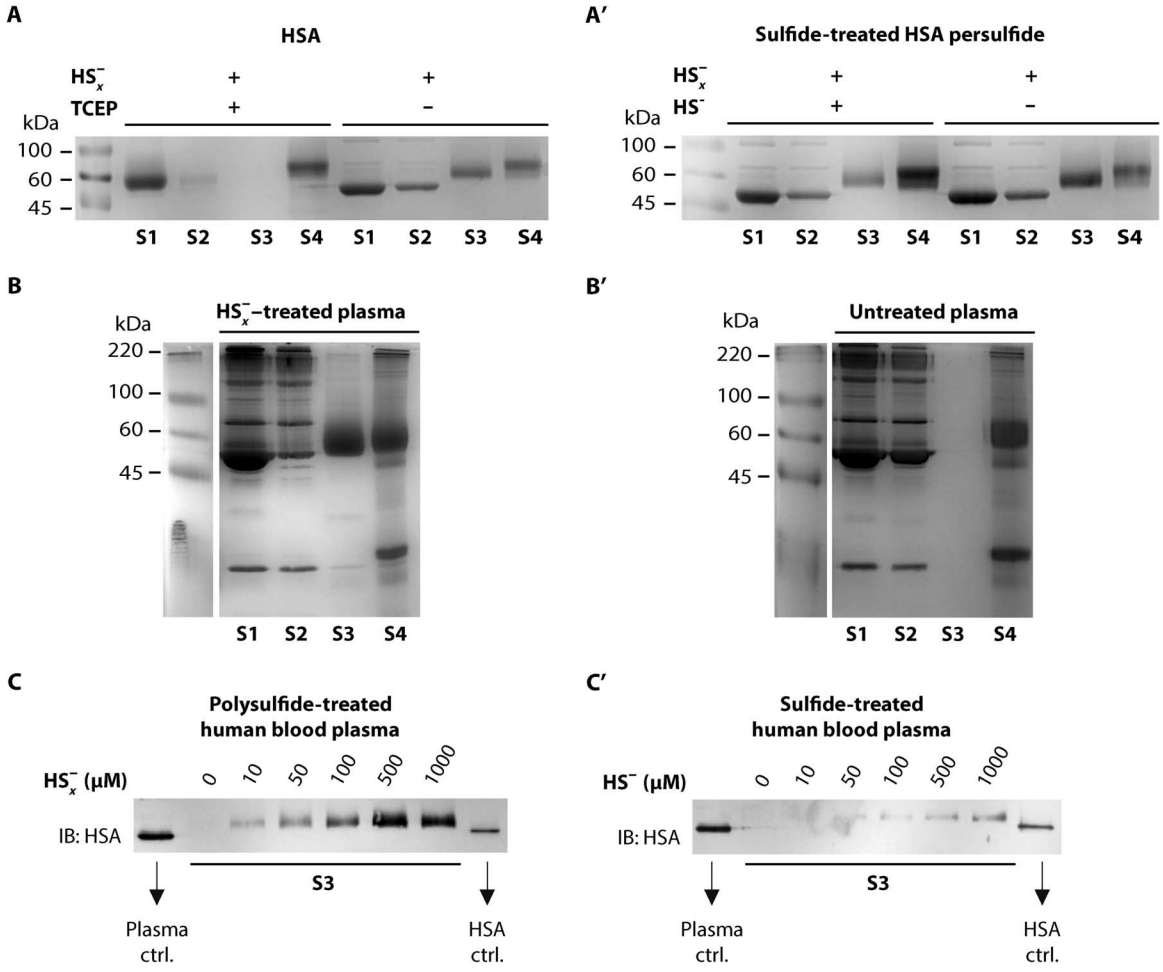

Fig. 2. Detection of protein persulfide formation on HSA. S1 to S4 refer to sampling according to Fig. 1. (**A**) IAB alkylated HSA-SSH samples are efficiently pulled down by streptavidin-coated magnetic beads (compare S1 to S2). Lanes S3 and S4 represent HSA-SSH that was reduced off the beads by TCEP and HSA thiol that was released during boiling, respectively. No bands were detected in S3 when HSA-SSH was reduced by TCEP before alkylation. Gels are representative of $n = 9$ experiments. (**A′**) Incubation of HSA-SSH with 5 mM sulfide for 30 min before alkylation reduces some of the HSA-SSH by shifting the equilibrium of reaction 1 (see text). (**B** and **B′**) HSA-SSH formation was observed in HS_x^--treated plasma samples (B), but no endogenous HSA-SSH was detectable in untreated plasma (B′) by Colloidal Coomassie Blue staining. Gels are representative of $n = 3$ experiments. (**C** and **C′**) Concentration-dependent (C) HS_x^- or (C′) H_2S treatment induced HSA-SSH formation in plasma detected by immunoblot analyses against HSA. Blots only show S3. Plasma protein (100 ng) and pure HSA (20 ng) were applied as loading controls. Blots are representative of $n = 3$ experiments. The observed mobility shifts on each gels are due to the reduction of structural disulfide bonds in HSA during the final reduction step. Mass spectrometry confirmed that the shifted bands indeed represent HSA.

persulfidation could indeed be detected at very high sulfide concentrations, this was most likely induced by an inevitable HS_x^- contamination (or formation of polysulfides during incubation) in the sulfide stock solutions, as shown previously for analyses of the active-site residues of PTEN (*23*).

Reduction of HS_x^- by the Trx system

Persulfidation is inhibitory for most thiol enzyme functions (*5*), but the effect of selenopersulfide (-SeSH) formation, to our knowledge, has not been tested for any functional selenocysteine (Sec)–containing enzyme. The Trx-reducing activities of mammalian TrxRs depend on a conserved solvent-exposed and highly reactive C-terminal Sec residue (*28*, *29*). Therefore, we investigated how HS_x^- exposure affects the activity of TrxR1. Instead of enzyme inhibition, we found that in the presence of its natural electron donor NADPH (reduced form of nicotinamide adenine dinucleotide phosphate), TrxR1 catalytically reduces HS_x^- in a polysulfide concentration–dependent manner (Fig. 3A). Both the zero-order character of the observed kinetic traces (reflecting efficient enzyme-catalyzed reactions) and the fact that substrate saturation could not be achieved using HS_x^- concentrations as high as 1 mM (Fig. 3B) indicated that HS_x^- are good substrates for TrxR1. To test a potential selenopersulfide formation–induced (or competitive inhibition–mediated) decline in TrxR1 activity in turnover with selenite as another low–molecular weight substrate of the enzyme (*30*), we added 50 μM selenite to the NADPH/TrxR1/polysulfide mixtures. No enzyme inhibition was detected; rather, an additive effect was observed in NADPH consumption rates (Fig. 3C and fig. S2), suggesting that the enzyme is not saturated under these conditions. These experiments clearly showed that polysulfides are substrates and not inhibitors of TrxR1.

We next assessed whether polysulfide reduction by TrxR1 was Sec-dependent using mutant variants of the enzyme. A Sec-to-Ser mutant was inactive (Fig. 3D), whereas a Sec-to-Cys mutant displayed about 5 to 10% turnover (fig. S3A) compared to the wild-type enzyme (Fig. 3A). Two other mutated variants of truncated TrxR1 lacking the Sec residue were also inactive (fig. S3, B and C), indicating that polysulfide reduction by the enzyme was dependent on its proper C-terminal active-site motif -GCUG and displayed at least 10-fold higher activity in the form of the native selenoprotein compared to a Sec-to-Cys substituted variant of the enzyme. These characteristics are typical for most natural TrxR1 substrates (*28*).

HS_x^- reduction rates were further increased upon addition of physiological concentrations of either Trx1 (5 μM) or TRP14 (2 μM) by 1.7- and 2.6-fold, respectively (Fig. 3E). Furthermore, addition of HS_x^- did not inhibit reduction of the alternative Trx1 substrate insulin (Fig. 3F) or the TRP14 substrate cystine (Fig. 3G); instead, similar additive effects were observed as in the selenite assay for TrxR1. These results demonstrated that the Trx system, comprising NADPH, TrxR1, and Trx1 or TRP14, provides a potent enzymatic system for the reduction of polysulfides.

Protein persulfide reduction by the Trx system

Next, we investigated whether protein persulfides can be reduced by the Trx system, first using bovine serum albumin persulfide (BSA-SSH) as a model substrate. BSA-SSH was produced and detected with ProPerDP as described for HSA (see fig. S4). TrxR1 alone as well as in a concerted manner with Trx1 and TRP14 could indeed reduce BSA-SSH. BSA-SSH was rapidly reduced using 50 nM TrxR1 and either 5 μM Trx1 or 2 μM TRP14 (Fig. 3H). Control experiments verified that the observed activities were not due to residual HS_x^- (used to generate BSA-SSH) remaining in the protein samples (fig. S5A) and that the catalytic reduction proceeded in a BSA-SSH concentration–dependent manner (fig. S5, B and C). With 5 μM Trx1 or 2 μM TRP14 accelerating the BSA-SSH reduction rates 1.7- and 2.4-fold, respectively, compared to TrxR1 alone, the protein persulfide reduction (just like for HS_x^-, see above) was most favorable via the TRP14-catalyzed pathway (Fig. 3H).

Protein persulfide detection in cells

To assess the impact of the Trx system on protein persulfide levels in a cellular context, we first validated ProPerDP for analyses of protein persulfides in cell lysates. For this, we generated a protein persulfide pool by treating lysates of A549 human lung carcinoma cells with HS_x^-, which revealed that a number of protein persulfide species could be detected upon polysulfide treatment that were below detection level in nontreated samples (Fig. 4A). The protein persulfide species present in the S3 sample again disappeared if the sample was treated with TCEP before the alkylation step (indicating no background signals even in cell lysates). To prevent artificial oxidation upon cell lysis, rapid alkylation of reactive thiol and persulfide groups in intact cells is necessary if protein persulfide analyses are to be done with live cells. This is enabled with ProPerDP because the biotin-tagged alkylating agent (IAB) readily crosses through cell membranes, demonstrated by the large amounts of proteins removed by the streptavidin-coated beads when the alkylating agent was used on intact cells and washed away in the cell culture before the cells were lysed (Fig. 4B, compare lanes S1 and S2). Most of these proteins could not be reduced off the beads using TCEP or dithiothreitol (DTT) (Fig. 4B, lane S4), thus representing proteins with free thiols and other Cys derivatives that could generate thioether bonds with the alkylating agent inside the cell (also see Fig. 1). The results shown in Fig. 4B also indicated that ProPerDP could be used to identify a small subset of proteins that formed persulfides upon HS_x^- treatment in intact cells (Fig. 4B, lane S3). Mass spectrometry–based identification of some of these proteins (Fig. 4, B and C, bands 1 to 4) gave closely overlapping results with proteins being previously reported as persulfidated by Ida *et al.* (*7*) and Mustafa *et al.* (*31*). However, considerably lower levels of endogenous protein persulfides were detected compared to those in HS_x^--treated samples. Even if silver staining was used with highly concentrated samples, the protein persulfides were only scarcely detectable in the untreated cell sample (Fig. 4D).

Using ProPerDP, we could also detect protein persulfides in yeast. Thereby, we were able to test the impacts of the two known sulfide-generating enzymes (*32*), which were also proposed to directly generate persulfide species, cystathionine-β-synthase (CBS) and cystathionine-γ-lyase (CSE) (*7*), on in vivo levels of protein persulfides. The observed lower levels of persulfidation in CBS- or CSE-deleted yeast strains compared to the wild-type mother cell line (Fig. 4E) were consistent with the known activities of these enzymes in generating intracellular H_2S, thereby providing another level of method validation.

Intracellular modulation of protein persulfide homeostasis by TrxR1 and TRP14

To assess whether the protein persulfide and/or HS_x^- reduction by the Trx system might have an impact on persulfide levels in a cellular context, we constructed stable TrxR1 and TRP14 knockdown human embryonic kidney 293 (HEK293) cell lines (Fig. 5A). Using ProPerDP, we found that HEK293 cells contained 1.52 ± 0.55 μg of endogenous basal levels of protein persulfides per milligram of protein, suggesting that 0.15 ± 0.06% (from $n = 3$ experiments) of the total proteins are persulfidated. ProPerDP detected 25 ± 9% and 29 ± 11% (mean ± SD from $n = 4$ experiments reaching statistical significance with $P < 0.05$; see Fig. 5, B and C) more total persulfidated proteins in the TrxR1- and TRP14-deficient HEK293 cells, respectively, compared to control cells [HEK293 cells transfected with a plasmid transcribing a scramble shRNA (short hairpin RNA)]. Control experiments verified that this was not due to less efficient alkylation or pulldown by the beads (fig. S6) and should thereby likely be explained by the lower reduction capacity of persulfide moieties in the cells deficient in TrxR1 or TRP14. In addition, HS_x^- treatment induced more protein persulfide formation in the deficient cells compared to control cells (Fig. 5D). We estimate that the level of protein persulfides in the polysulfide-treated control cells is >3 μg/mg total protein, which is ~2.7- and ~3.7-fold larger in the TrxR1 and TRP14 knockdown cells, respectively, based on Fig. 5D. Dose-dependent treatment of intact cells with toxic amounts of HS_x^- for 2 hours resulted in significantly lowered viability of TrxR1-deficient cells compared to control cells at 24 hours after treatment (Fig. 5E). These observations collectively show that the Trx system is involved in intracellular reduction of protein persulfide species and in the maintenance of cellular sulfane sulfur homeostasis.

Polysulfide and protein persulfide reduction by the GSH system

Working hand in hand with the Trx system, the GSH system serves as the other major disulfide-reducing machinery in vivo (*33*). Therefore, we also investigated its potential to reduce polysulfide and protein persulfide species. Using NADPH and GSH, GR catalyzed the reduction of HS_x^- in a concentration-dependent manner (Fig. 6A). Inclusion of Grx in the enzyme kinetic assay further increased catalytic power (Fig. 6B).

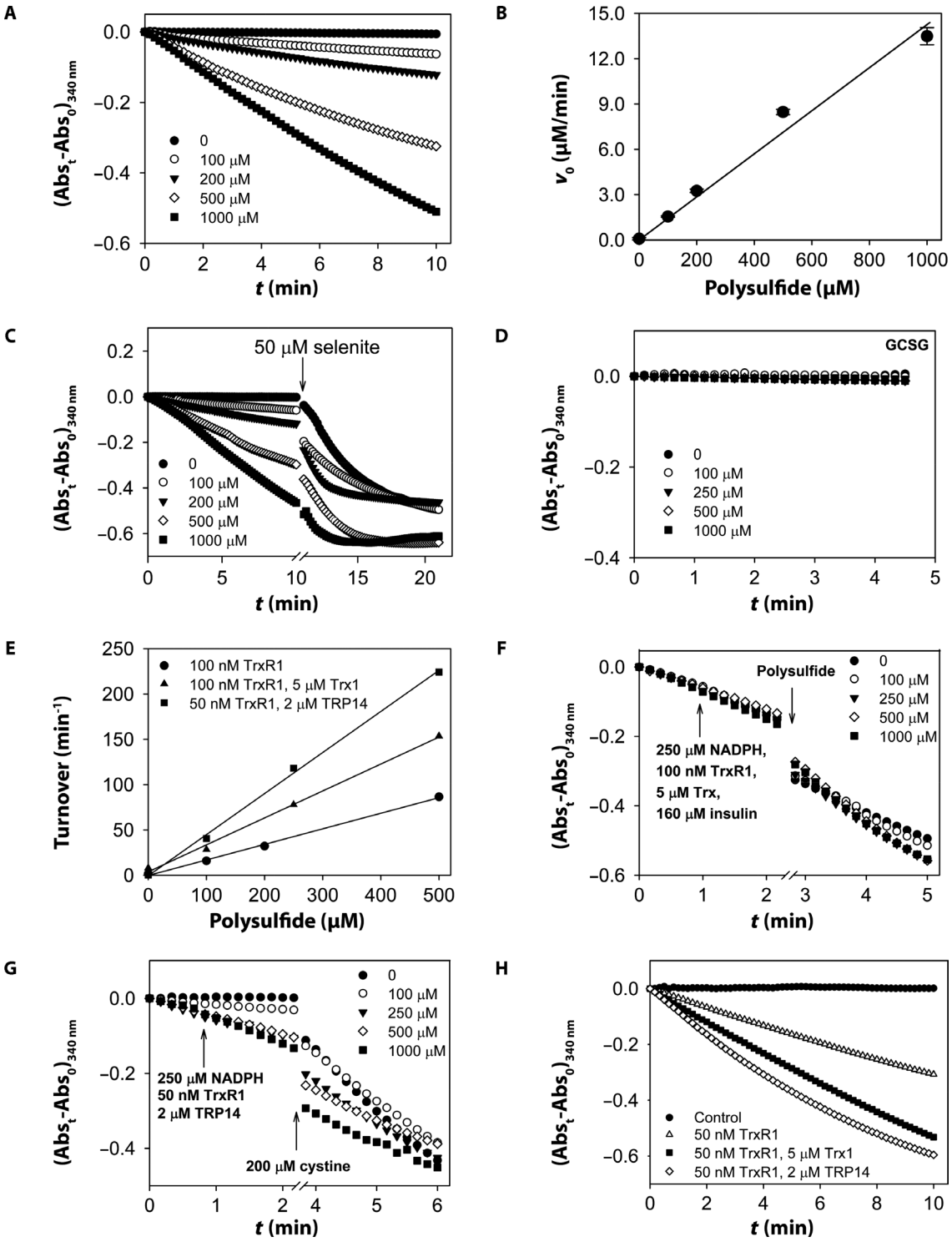

Fig. 3. Catalytic reduction of HS_x^- and BSA-SSH by the Trx system. (**A**) Kinetic traces show catalytic reduction of increasing concentrations of HS_x^- at 100 nM TrxR1 and 250 μM NADPH following the consumption of NADPH (at 340 nm). (**B**) Initial rates of NADPH consumption by TrxR1 using HS_x^- as substrate show linear dependence on the HS_x^- concentration up to 1 mM. (**C**) Addition of 50 μM sodium selenite (at the indicated time point by the arrow) to similar reaction mixtures as in (A) resulted in increased NADPH consumption rates (also see fig. S2). (**D**) The GCSG mutant of TrxR1 is inactive in a similar activity assay as in (A), indicating the need for catalysis of the Sec residue (see the activities of further mutants in fig. S3, A to C). (**E**) TrxR1 concentration–corrected initial rates were increased in the presence of 5 μM Trx1 and 2 μM TRP14 compared to TrxR1 alone with linear HS_x^- concentration dependencies. (**F** and **G**) Addition of HS_x^- had no inhibitory potential on TrxR1-coupled (**F**) insulin-reducing Trx1 activities or (**G**) cystine-reducing TRP14 activities. (**H**) Kinetic traces show catalytic reduction of 170 μM BSA-SSH by 50 nM TrxR1 at 250 μM NADPH, which are further accelerated by 5 μM Trx1 or 2 μM TRP14.

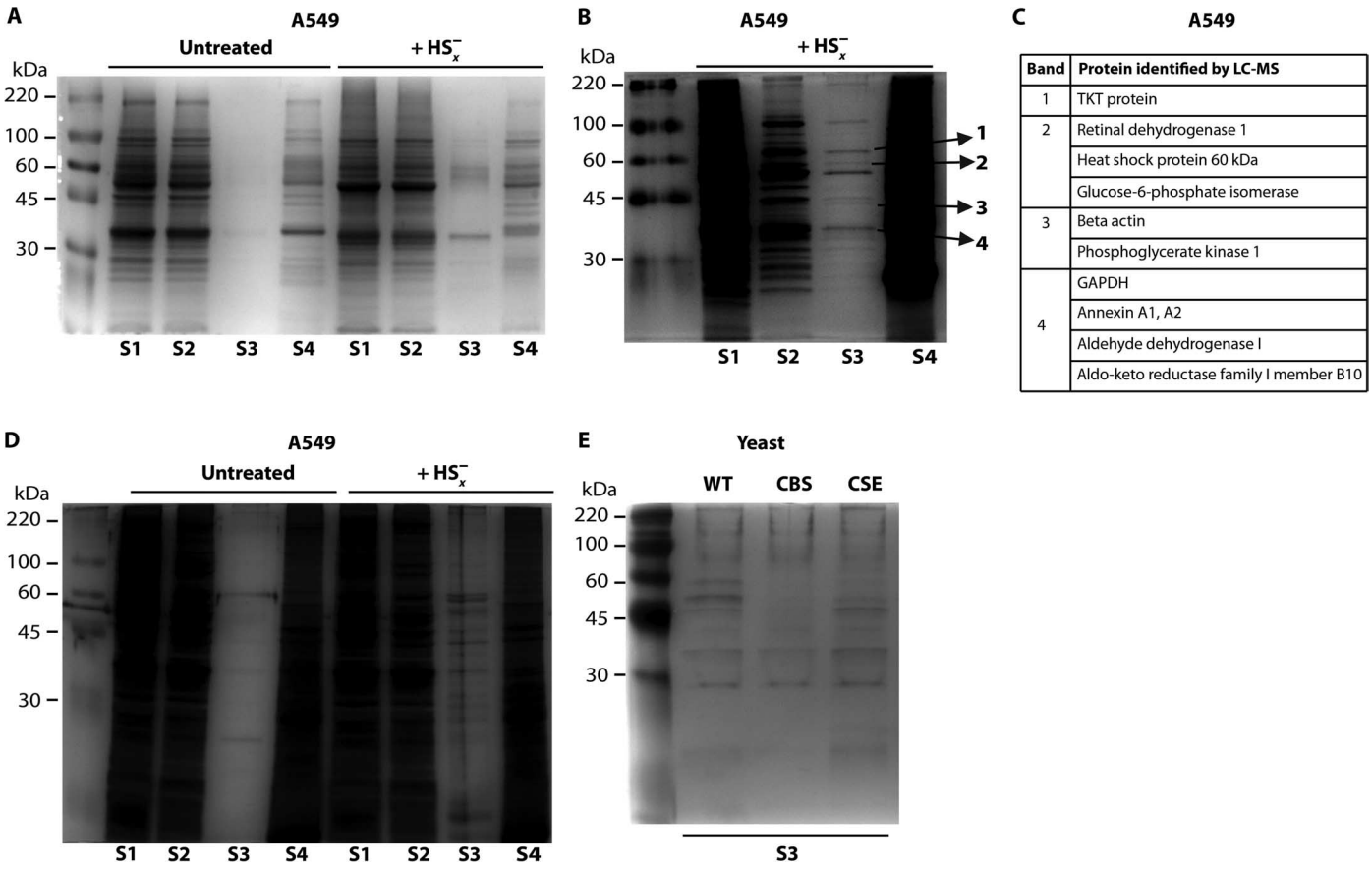

Band	Protein identified by LC-MS
1	TKT protein
2	Retinal dehydrogenase 1
	Heat shock protein 60 kDa
	Glucose-6-phosphate isomerase
3	Beta actin
	Phosphoglycerate kinase 1
4	GAPDH
	Annexin A1, A2
	Aldehyde dehydrogenase I
	Aldo-keto reductase family I member B10

Fig. 4. Protein persulfide detection in cells. S1 to S4 refer to sampling according to Fig. 1. (**A**) Detection of persulfides in HS_x^--treated and untreated A549 cell lysates (Coomassie staining). (**B**) Persulfide detection in HS_x^--treated intact A549 cells, where the alkylating agent is washed away before the cell lysis step, as visualized by Coomassie staining. The indicated bands in S3 were subsequently subjected to tryptic digestion and mass spectrometry analyses. (**C**) List of identified persulfidated proteins from the bands indicated on (B). (**D**) Endogenous persulfidation can only be visualized by silver staining. Gels are representative of $n = 3$ experiments. (**E**) More protein persulfides were detected in wild type (WT) compared to *cys4*Δ and *cys3*Δ yeast strains representing the corresponding CBS and CSE deleted variants, respectively. For sample preparation and the relevant genotypes, see Materials and Methods.

Up to 1 mM HS_x^-, linear concentration dependencies were observed for the catalyzed reduction rates in both assays, suggesting that polysulfides are good substrates for these enzyme systems (Fig. 6C). Similar to the Trx system, using BSA-SSH, we found that, in the presence of NADPH, GR together with GSH has the potential to catalytically reduce protein persulfide species, with substantially increased reduction rates in the coupled assay with Grx (Fig. 6D). As above, control experiments verified that the observed activities were not due to residual HS_x^- (which were used to generate BSA-SSH) remaining in the protein samples (fig. S7).

In vivo orchestration of protein persulfidation by Trx and GSH systems

To investigate the in vivo significance of the persulfide- and HS_x^--reducing potentials of the Trx and GSH machineries, we further developed ProPerDP to detect protein persulfides in tissue samples (see Materials and Methods for details). Using an analogous protein quantification protocol to the one used for the cellular systems, ProPerDP measured 11.6 ± 6.9 μg of protein persulfides per milligram of total protein in the liver of 8- to 10-week-old wild-type male mice ($n = 8$ different animals). We observed different protein persulfidation patterns in mouse livers engineered (*34*) to lack GR (GR-null) or to lack both TrxR1 and GR (TR/GR-null) in hepatocytes as compared to matching wild-type livers (Fig. 7A). Furthermore, significantly ($P = 0.02$) elevated persulfide levels, 20.2 ± 9.0 μg/mg of total protein, were observed in TR/GR-null liver samples compared to wild type (Fig. 7B). These observations give credence to the important role of the protein persulfide- and/or HS_x^--reducing activities of the Trx and GSH systems in governing sulfane sulfur homeostasis and sulfide signaling in vivo.

DISCUSSION

Here, we presented a novel method, ProPerDP, for analysis of protein persulfide species. We characterized catalytic reduction of such entities by the Trx system, and we used ProPerDP to show that TrxR1 and TRP14 expression have an impact on protein persulfide accumulation in cells. TrxR1 knockdown cells were less viable in the presence of toxic amounts of HS_x^-, providing corroborating evidence for the physiological importance of an intact Trx system to maintain intracellular sulfane sulfur homeostasis. The Grx/GR/GSH system was also found to be capable of catalytically reducing polysulfide and protein persulfide species. The significantly elevated levels of protein persulfides that were detected in TR/GR-null livers compared to wild-type livers underline the importance of these reducing systems in protein persulfidation mechanisms in vivo.

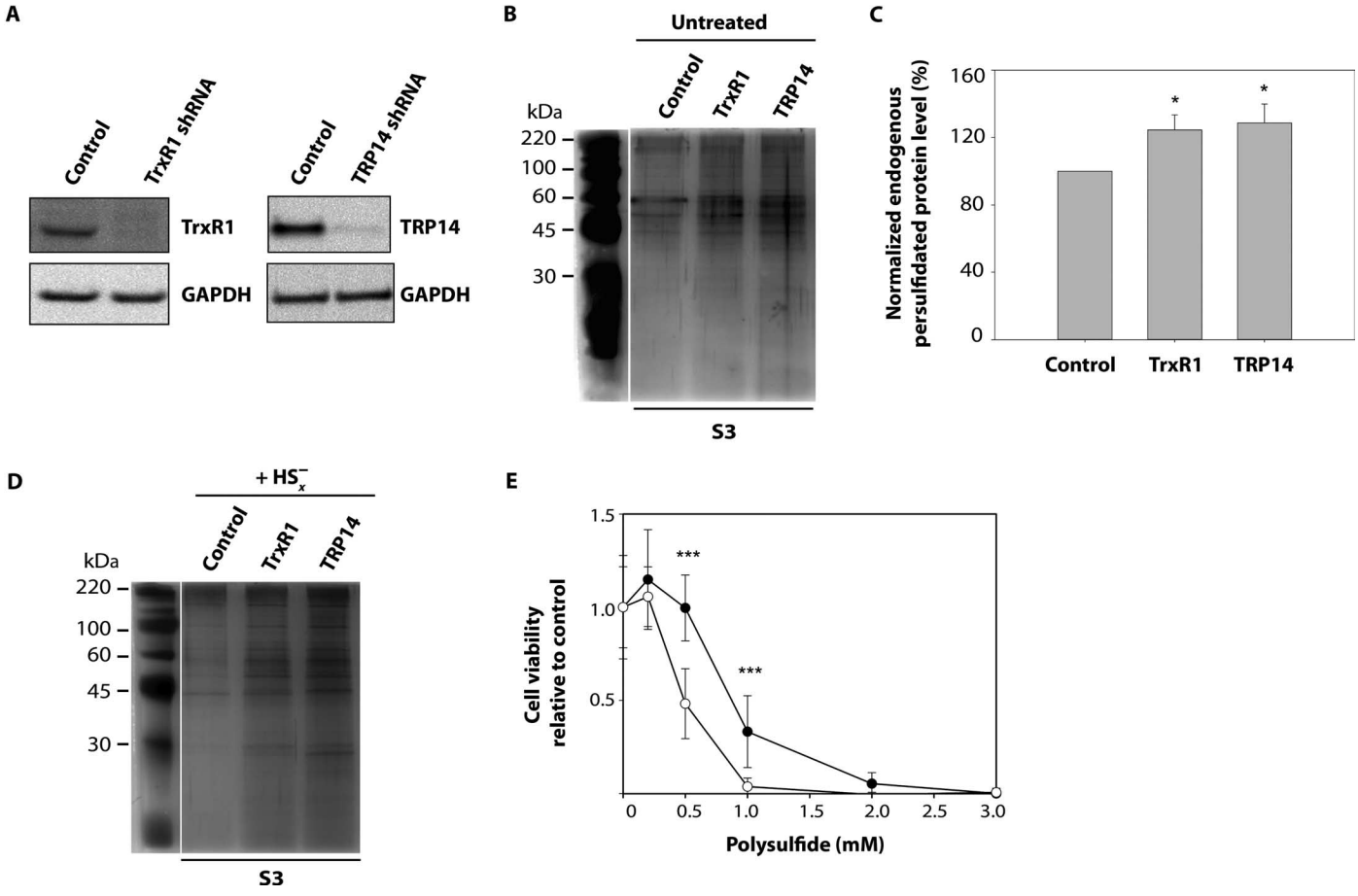

Fig. 5. TrxR1 and TRP14 counteract intracellular protein persulfide accumulation. S3 refers to sampling according to Fig. 1. (**A**) Western blot showing the knockdown of TRP14 and TrxR1 in stably transfected HEK293 cells, compared to control cells. GAPDH is applied as a loading control. (**B**) Representative silver-stained gel (of $n = 4$ experiments) shows that more protein persulfides are detected in TrxR1 and TRP14 knockdown HEK293 cells than in the control (control cells have been transfected with a plasmid that transcribes a scramble shRNA) under normal growth conditions. (**C**) Increases in protein persulfide levels in TrxR1 and TRP14 knockdown HEK293 cells compared to control reached statistical significance (*$P < 0.05$ using the paired t test); 100% in the control cells corresponds to 1.52 ± 0.55 μg/mg total protein. Error bars represent SDs of $n = 4$ experiments. (**D**) Two hours of treatment with 200 μM polysulfide induced higher levels of intracellular protein persulfides in intact TrxR1 and TRP14 knockdown cells compared to control cells. (**E**) A modified SRB cytotoxicity assay revealed that control cells (•) are significantly more viable upon polysulfide exposure than TrxR1 knockdown (○) cells (***$P < 0.0001$ at 0.5 and 1 mM polysulfide concentration). Data points and error bars represent the average and SD, respectively, of $n = 4$ independent experiments of triplicate measurements.

Moreover, the different patterns of persulfidated proteins we observed in wild-type, GR-null, and TR/GR-null livers by gel electrophoresis of ProPerDP-captured products suggest that there are different specific roles for the Trx and GSH systems in governing persulfide reduction pathways. These findings have several implications for the understanding of H_2S signaling through protein persulfide formation and function.

Since the discovery by Snyder's group that protein persulfidation, also called sulfhydration, is a major pathway in sulfide signaling (*31*), a number of elegant studies have shown that protein Cys persulfide formation can have regulatory functions. Examples include (i) antiapoptotic transcriptional activity triggered by persulfide-mediated binding of ribosomal protein S3 (RPS3) to nuclear factor kappa-light-chain-enhancer of activated B cells (NF-κB) (*35*), (ii) extracellular signal–regulated kinases 1/2 (ERK1/2) translocation into the nucleus facilitated by mitogen-activated protein kinase kinase (MEK1) persulfide formation–induced poly(ADP-ribose) polymerase 1 (PARP-1) activation leading to DNA damage repair (*36*), (iii) adenosine triphosphate (ATP)–sensitive channel activation upon persulfide-induced inhibition of ATP binding (*37*), and (iv) potent inhibition of PTEN (*23*) or of protein-tyrosine phosphatase 1B (PTP1B) (*20*) activities by persulfidation of their active-site Cys residues. In addition, a thiol protein–protecting effect by persulfidation was recently suggested, because persulfide moieties are in theory reducible oxidative modifications as opposed to irreversible oxidation of Cys thiols (*7*, *14*, *23*). Our results suggest not only that both Trx and GSH systems participate in the regeneration of such protective modifications but also that these reducing machineries may thereby be involved in the regulation of a subset of many key proteins that are regulated by persulfide formation. Additional studies are required to assess such regulations in a protein-specific manner, but a general discussion of potential models is already possible at this stage (see below).

One important question with regard to protein persulfide modifications as regulatory mechanisms for cell function is how common such modifications are and at what levels protein persulfides accumulate in cells. Although a few persulfide assays were published recently, detection

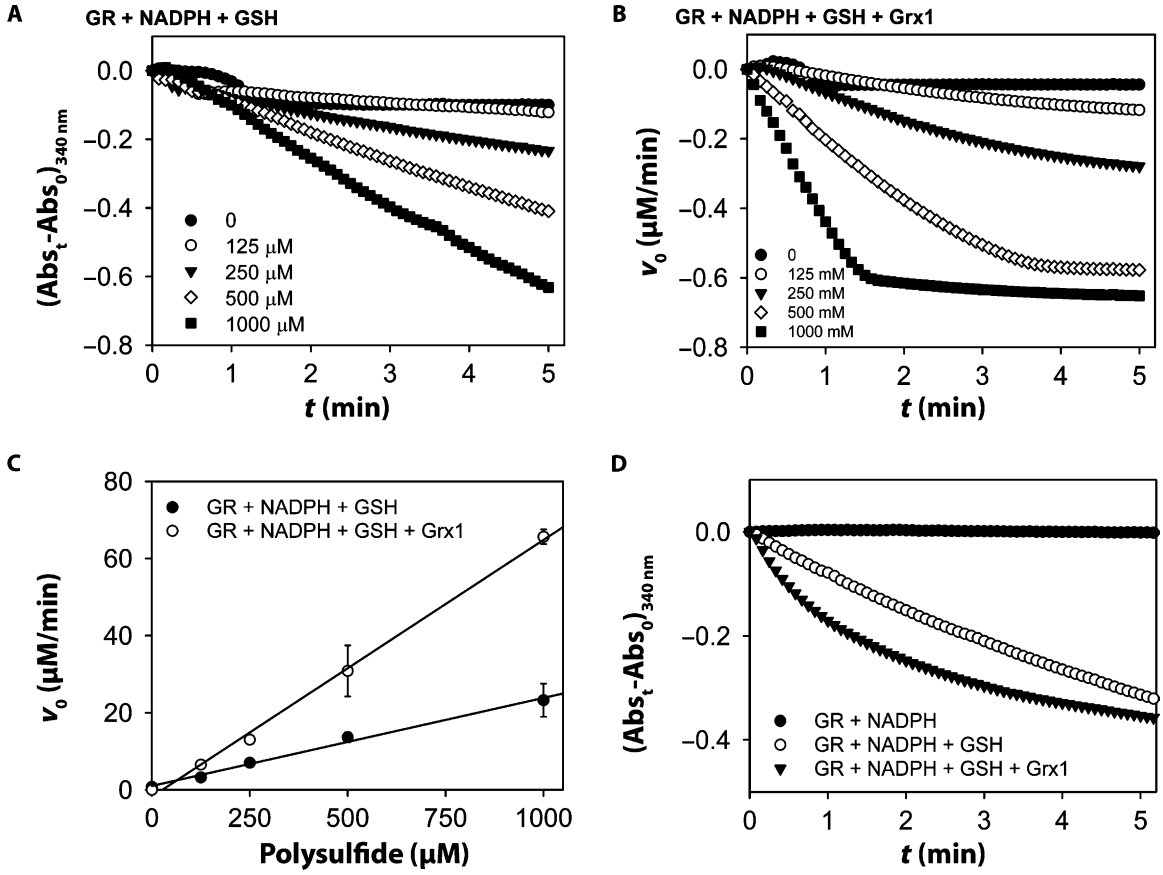

Fig. 6. Catalytic reduction of HS_x^- and BSA-SSH by the glutaredoxin system. (**A** and **B**) Kinetic traces show catalytic reduction of increasing concentrations of HS_x^- at 6 μg/ml GR, 250 μM NADPH, and 1 mM GSH in the absence (A) or presence (B) of 1 μM Grx1 following the consumption of NADPH (at 340 nm). (**C**) Initial rates of NADPH consumption by the GSH system using HS_x^- as a substrate in the enzyme systems described in (A) and (B), represented by "•" and "○" symbols, respectively, show linear dependence on the HS_x^- concentration up to 1 mM. (**D**) Kinetic traces show catalytic reduction of 170 μM BSA-SSH at 6 μg/ml GR, 250 μM NADPH, and 1 mM GSH in the absence or presence of 1 μM Grx1.

and quantification of intracellular protein persulfidation have remained problematic. The most extensively used assays thus far have been the modified biotin switch (*31*) and the recently published tag-switch (*7*, *38*) methods. The modified biotin switch method is based on the assumption that methyl methanethiosulfonate (MMTS) selectively blocks thiols over persulfides, which, however, has been questioned a number of times on chemical grounds (*38*, *39*). In fact, at pH 7, many persulfides were suggested to be even better nucleophiles than the corresponding thiol moieties (*14*) and would hence be expected to react faster with alkylating agents (such as MMTS). In the tag-switch assay, methylsulfonyl benzothiazole (MSBT) (the alkylating agent) is not permeable for cell membranes, which excludes the possibility of persulfide detection in intact live cells. Furthermore, in the "switching" step, methyl cyanoacetate was suggested to selectively cleave MSBT-labeled dialkyl disulfides (generated by alkylation of persulfide species) over protein disulfide moieties. However, selectivity was only assessed on the *N-tert*-butyloxycarbonyl derivatized cystine and on glutathionylated bovine serum albumin (BSA), not taking into account the presence of activated functional disulfides in cellular systems, which exhibit orders of magnitude larger reactivities (*40*). For example, protein disulfide isomerase (PDI) persulfidation could potentially represent a false-positive hit in the tag-switch assay, because this oxidoreductase uses an activated disulfide moiety in its active site to introduce disulfide bonds in newly synthesized polypeptides in the endoplasmic reticulum (ER) (*40*). On the other hand, that reactivity of the PDI disulfide could also potentially be responsible for its persulfidation by a direct reaction with sulfide in the ER (*25*). These examples and uncertainties demonstrate that a new method to determine intracellular persulfide formation has been highly desired, which was the basis for our development of ProPerDP. It should be noted that in A549 cells, we identified a limited number of proteins that were prominently persulfidated upon treatment with HS_x^- that all contain a redox-sensitive Cys residue, and most of these proteins were also picked up by the tag-switch or by the modified biotin switch assays (*7*, *31*). In light of the estimated 20 mM total intracellular Cys concentration (*41*, *42*) and the fact that most mammalian proteins have at least one Cys residue (*43*), the quantified ~0.1 to 1% persulfidation of the total protein pool in cells (1.52 ± 0.55 μg/mg total protein in HEK293 cells) and liver tissue (11.6 ± 6.9 μg/mg total protein in mice), respectively, correlates very well with the ~10 to 100 μM small-molecule persulfide (mostly GSH persulfide) concentrations in A549 cells and mouse liver, respectively, that were measured by Ida *et al.* (*7*).

We need to point out that the ProPerDP method is not without caveats either. Some proteins have more than one surface-exposed thiol residue, some of which might form persulfides more preferentially than

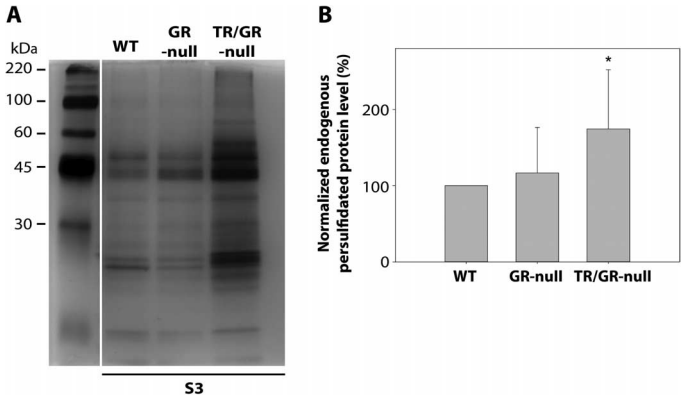

Fig. 7. Trx and GSH systems orchestrate protein persulfide levels in vivo. (**A**) Representative silver-stained gel demonstrates the detected differences in protein persulfide pools of liver samples from mice engineered to lack GR (GR-null) or TrxR1 and GR (TR/GR-null) in hepatocytes compared to that of an age-matched healthy control (WT). S3 refers to sampling according to Fig. 1. (**B**) Increased levels of protein persulfides were detected by ProPerDP (see Materials and Methods) in GR-null and TR/GR-null mouse liver samples compared to WT, reaching statistical significance (*P < 0.05 using nonpaired t test) for TR/GR-null; 100% in the WT animals corresponds to 11.6 ± 6.9 μg/mg total protein (n = 7 different animals). Error bars represent SDs of n = 8 experiments with different animals for TR/GR-null and n = 5 for GR-null.

others. Proteins in which a free thiol is alkylated at the same time as a persulfide group is present at another site may be lost in our assay (Fig. 8A). Another caveat with our method is that it could potentially detect disulfide-linked proteins in which an extra surface-exposed nonpersulfidated free Cys residue (in the absence of denaturation) also becomes alkylated (Fig. 8B). However, the fact that the levels of most of the detected endogenous persulfidated proteins increased in A549 or HEK293 cells (see fig. S8) upon HS_x^- treatment suggests that only a small proportion (if at all) of the observed bands are due to such false-positive hits. In addition, using two-dimensional (2D) diagonal gel electrophoresis (with a nonreducing and a reducing dimension), we could not detect significant differences in the intermolecular disulfide pools of the S1 and S2 fractions (fig. S9; see Fig. 1 for an explanation of fractions), corroborating that false-positive hits by ProPerDP via the above mechanism (Fig. 8B) are likely minor. Furthermore, the fact that reduced protein persulfide levels were observed in CBS- or CSE-deleted yeast cells compared to the wild-type mother strain verifies that ProPerDP indeed detects protein persulfide species. However, it has to be noted that, in its current form, ProPerDP cannot distinguish between protein persulfides and protein polysulfide species. Therefore, we advise investigators to be cognizant of the abovementioned limitations when running the assay. A potential methodological improvement using mass spectrometry–based detection to overcome the abovementioned caveats (as argued above, with the false-negative hits being more relevant) is proposed in Fig. 8C. This includes trypsinization before the affinity purification step, because on the peptide level, situations outlined in Fig. 8 (A and B) would become highly unlikely.

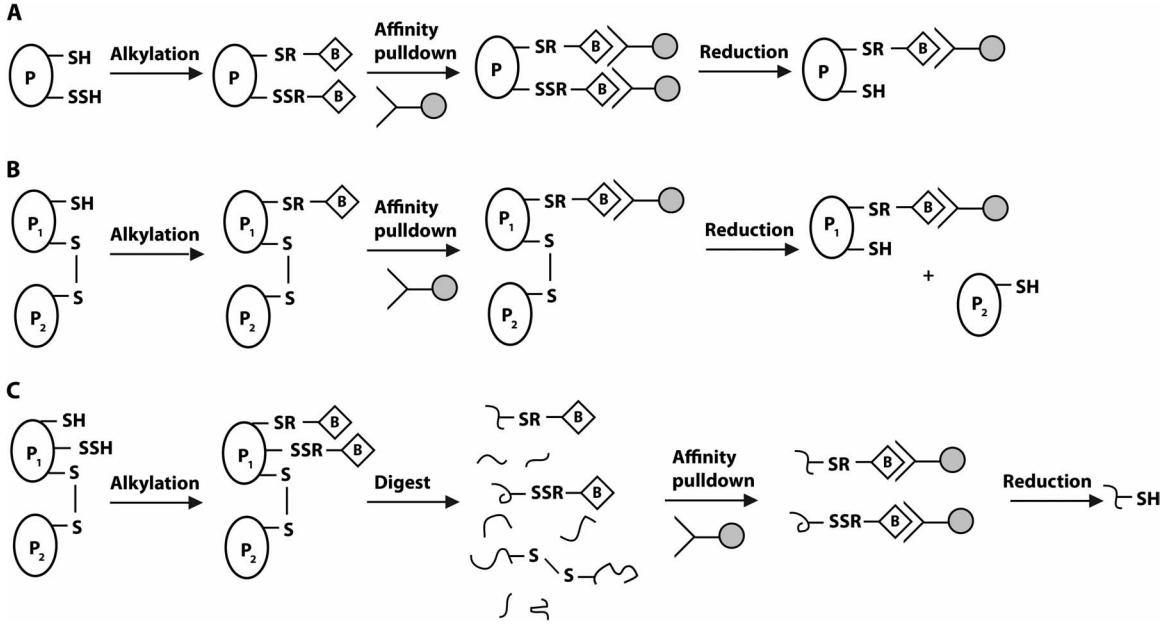

Fig. 8. Potential caveats of the ProPerDP method. (**A**) In proteins with more than one free Cys that exhibit different persulfidation properties, because of a nonpersulfidated Cys residue, the protein can stay immobilized on the streptavidin beads despite containing a persulfide, leading to false-negative signals. (**B**) Intermolecular protein disulfide bonds with nonpersulfidated extra Cys residues on one of the polypeptide chains might appear as false-positive signals in the persulfide proteome. Upon reduction, P_2 proteins are cleaved off the beads and could erroneously be present in the persulfide proteome fractions (Sample 3 in Fig. 1). (**C**) A potential way to overcome the abovementioned caveats is to digest the alkylated proteins before the pulldown step because it is highly unlikely that both the free and persulfidated Cys [for (A)] or the disulfide and the free Cys moieties [for (B)] will end up in the same peptide using this method. With this approach, the alkylated peptide persulfides could be detected by mass spectrometry after they are cleaved off the beads by the reducing agent. This method improvement is under development in our laboratory.

Possible mechanisms of protein persulfide formation via sulfide or Cys thiol oxidation processes (*5*) as well as enzymatic pathways (*7*, *32*) are being extensively studied. By contrast, counteracting pathways for reduction of protein persulfide species are much less well understood. Recent reports from Kimura's and Tonks' laboratories have suggested that 3-mercaptopyruvate sulfurtransferase and PTP1B persulfides are likely to be reduced by Trx1, on the basis of their observed faster reduction rates compared to DTT, GSH, or dihomo-γ-linoleic acid, using purified enzymes and cell lysate experiments (*19*, *20*). However, to the best of our knowledge, no mechanistic studies or analyses have been conducted to date with regard to reduction pathways for either protein persulfides or polysulfides (HS_x^-) in intact cells or tissue samples. Here, we used enzyme kinetic studies to demonstrate that TrxR1 catalyzes the direct reduction of HS_x^- as well as protein persulfide moieties via its Sec residue. Further catalytic power is introduced in the presence of physiological concentrations of Trx1 or TRP14. In contrast to most thiol proteins (see above), the fact that HS_x^- did not inhibit the activities of either TrxR1, Trx1, or TRP14 suggests that any TrxR1 selenopersulfide and Trx1 or TRP14 persulfide intermediate species (that should form during the reduction process; fig. S10) are rapidly reduced by the resolving Cys residues in the active sites of TrxR1, Trx1, or TRP14.

Perhaps our most important finding with regard to the reduction of protein persulfides by the Trx system is that TRP14 is an efficient catalyst. TRP14 is a newly discovered member of the Trx protein family that lacks activity with typical Trx substrates such as ribonucleotide reductase, insulin, or peroxiredoxins (*21*). The protein was, however, recently found to support cystine and nitrosothiol reduction (*22*) and can also reactivate oxidized PTP1B (*44*). The latter property of TRP14 becomes even more interesting in light of our findings that TRP14 is a prominent protein persulfide reductase, because PTP1B has also been found to be regulated by persulfidation (*20*). Hence, TRP14 is emerging as a very efficient substrate of TrxR1 (*22*) that may be specifically tailored for redox signaling purposes. Indeed, particularly under increasingly oxidizing or proliferating growth conditions, during which Trx would be heavily engaged in turning over the peroxiredoxin system (*45*) or providing electrons for ribonucleotide reductase (*46*), TRP14 is likely to be the major regulator of protein persulfide levels because its activity is not affected by the presence of protein disulfide substrates that are reduced by Trx1 but not by TRP14 (*22*).

Demonstrating the physiological importance of the Trx system for protein persulfide reduction, the ProPerDP method here allowed us to measure increased endogenous protein persulfide levels in intact HEK293 cells upon knockdown of TrxR1 or TRP14. Furthermore, polysulfide treatment induced accumulation of higher protein persulfide levels in deficient cells, and TrxR1 knockdown cells were significantly more susceptible to toxic amounts of HS_x^- compared to control cells. These observations highlight that TrxR1 and TRP14 should indeed be considered major players in the cellular pathways that maintain sulfane sulfur homeostasis.

In addition to roles for the various components of the Trx system in modulating protein persulfidation, we here report that the GSH system can also reduce inorganic HS_x^- and protein persulfides. This activity is enzymatically enhanced by inclusion of Grx and represents an independent mechanism of modulating the cellular persulfide milieu via an NADPH-dependent reductase system. Although this might represent yet another physiological process wherein the Trx and GSH systems robustly overlap with each other, some of our data suggest that the two systems might act independently to fine-tune the protein persulfide response. Thus, we found that a distinct subset of proteins are targets for persulfide accumulation in wild-type, GR-null, or TR/GR-null liver samples, suggesting that the persulfide-reducing capacities of the Trx and GSH systems might be protein persulfide–specific and potentially involved in different signaling pathways. Further studies will be required to understand the detailed molecular mechanisms by which such systems mediate H_2S signaling functions and the respective roles of the Trx and GSH systems in these processes. The significantly increased and altered levels of protein persulfides observed in the TR/GR-null mouse liver samples emphasize the orchestrating role of the Trx and GSH systems in reducing protein Cys persulfides in vivo.

MATERIALS AND METHODS

Reagents

All chemicals were analytical reagent grade or better and purchased from Sigma-Aldrich, unless indicated otherwise. Sulfide stock solutions were prepared fresh daily in water using $Na_2S{\cdot}9H_2O$ (ACS reagent, ≥98%). Sulfide concentrations were determined by two different ultraviolet (UV)–vis spectrophotometric methods, as described previously (*25*). Sodium hypochlorite concentration was determined at 292 nm ($\varepsilon = 350\ M^{-1}\ cm^{-1}$). Polysulfide stock solutions were prepared by dropwise addition of NaOCl stock solution to sulfide stock solution, at a final concentration ratio of 100 mM HS^-/30 mM NaOCl in double-distilled H_2O, under vigorous vortexing conditions to avoid sulfur precipitation, as reported previously (*47*). Polysulfide reagent solutions (in which polysulfide/sulfide ratios were ~3:4 for the preparation of HSA-SSH and ~1:3 for the cell experiments) were prepared by dilution of stock solutions with TE buffer (100 mM tris-HCl and 2 mM EDTA, pH 7.5). Polysulfide stock solutions were used within 30 min from preparation.

IAB is a product of Thermo Scientific. Streptavidin-coated magnetic microparticles were purchased from Sigma or Life Technologies (Dynabeads M-280). Streptavidin agarose resin from Thermo Scientific was used for the detection of BSA persulfide (fig. S4).

Protein expression and purification

Rat TrxR1 was expressed in *Escherichia coli* BL21 (DE3) gor^- strains cotransformed with $pETTRS_{TER}$ and pSUABC plasmids (*48*). Four TrxR1 mutants with regard to the C-terminal active site of TrxR1 (-GCUG), including a Sec-to-Cys or a Sec-to-Ser mutant (-GCCG or -GCSG), a truncation mutant (-GC), and a combination of truncation and Cys-to-Ser mutant (-GS), were used in this study and have been described previously (*49*). The corresponding plasmids were transformed into the same *E. coli* strain, and we used a "2.4/24/24" protocol for all TrxR1 variant protein expression (*50*, *51*). TrxR1 and its mutants were affinity-purified from 2′5′-ADP Sepharose (GE Healthcare) followed by size-exclusion chromatography using a Superdex G200 column equipped on an ÄKTA Explorer 100 workstation (GE Healthcare). Pure TrxR1 proteins were concentrated using a Centriprep Centrifugal Filter Unit with Ultracel-30 membrane (Millipore), and the concentration was determined by measuring flavin adenine dinucleotide (FAD) absorbance at 463 nm ($\varepsilon = 11{,}300\ M^{-1}\ cm^{-1}$); The Bradford method (Bio-Rad) was also used to make sure that each subunit of the TrxR1 variants contains one FAD molecule. The specific activity of the enzyme stock solution of the normal Sec-containing TrxR1 variant used in this study was 9.75 U/mg.

Human Trx1 was expressed in *E. coli* Stellar strain (Clontech). The coding region of Trx1 was codon-optimized for protein expression in *E. coli* and synthesized (DNA2.0). A His-tag followed by a tobacco etch virus (TEV) protease recognition site was introduced at the N-terminal

end of Trx1 for the convenience of purification. The protein was expressed conventionally and purified using immobilized metal affinity chromatography (IMAC). The His-tag was removed using TEV protease (*52*) and the nontagged Trx1 was eventually separated from the cleavage reaction mixture by running a counter-IMAC. The purified Trx1 was stored in TE buffer and concentrated using a Centriprep Centrifugal Filter Unit with Ultracel-3 membrane (Millipore), with the protein concentration determined by calculating from its UV absorbance at 280 nm (ε = 6970 M^{-1} cm^{-1}). Recombinant TRP14 was expressed and purified as previously described (*22*).

Preparation of HSA-SSH and BSA-SSH samples

Reduction of Cys residues on single-protein or complex biological samples (1 to 10 mg/ml protein), where indicated, was achieved by incubation with 1 mM TCEP in 100 mM tris-HCl/2 mM EDTA buffer at pH 7.5 (TE) for 30 min (prereduction step). TCEP was removed from the samples by Zeba Desalting Spin Columns (0.5 ml, 7K MWCO). Persulfide formation was induced by the addition of 10 mM HS^-/3 mM NaOCl to the samples [incubation in the dark at room temperature (RT) for 30 min]. Residual polysulfides were removed by gel filtration using Zeba Desalting Spin Columns (0.5 ml, 7K MWCO).

Treatment of human plasma samples by sulfide or polysulfides

Peripheral venous blood was obtained from healthy adult humans with informed consent. The procedure was approved by the Hungarian National Ethics Committee under file number BPR-021/00084-2/2014. Blood samples were collected into EDTA collection tubes and centrifuged at 3000 rpm for 10 min. The supernatant plasma was aliquoted into equal volumes, and protein content was determined by the Bradford assay (Bio-Rad). The total protein concentration of plasma samples fell into the 89.6 ± 11.6 mg/ml range. Samples were diluted to 10 mg/ml and treated with the indicated amount (for Fig. 2, C and C′) or with 3 mM polysulfide reagent or buffer (for Fig. 2, B and B′) in the dark at RT for 30 min, desalted by Zeba 7K MWCO Desalting Spin Columns (Thermo Scientific), and then alkylated by 1 mM IAB for 1 hour (Fig. 2, C and C′). After the alkylation, the ProPerDP method was applied to the plasma samples.

The ProPerDP method for purified protein samples

Desalted protein solutions were split into two aliquots of equal volume and incubated with or without 5 mM TCEP for 30 min at RT followed by alkylation with 1 mM IAB (3 hours at RT). The excess IAB was removed by gel filtration and by ultrafiltration using Amicon microconcentrators (Merck) or by dialysis overnight against TE buffer (using Pur-A-Lyzer Mini 12000 Dialysis Kit, Sigma). Biotinylated proteins were pulled down by streptavidin-coated magnetic beads (Sigma). After a 30-min incubation step on a shaking table, magnetic beads were separated from the solution phase with a magnetic particle separator (Dynal MPC-M). The supernatant was placed in a clean tube, and the beads were washed three times with tris-buffered saline containing 0.05% Tween 20 (TBST) to eliminate nonspecific adhesion. The beads were then resuspended and incubated with 5 mM TCEP (30 min, gentle mixing). The magnetic separation was repeated and the beads were finally boiled at 100°C for 3 min in SDS-PAGE sample loading to elute all bound material. The samples were then analyzed by SDS-PAGE gel electrophoresis or Western blot analyses and/or mass spectrometry depending on the composition and concentration conditions of the original sample. Protein concentrations were monitored throughout the process by the Bradford assay using the Bio-Rad protein reagent.

Protein persulfide detection in intact cells by ProPerDP

A549 or HEK293 cells were incubated in the presence or absence of 200 μM polysulfide in Hanks' balanced salt solution (HBSS; Lonza) for 30 min or 2 hours (in Fig. 5D) at 37°C, after which cells were rinsed with phosphate-buffered saline (PBS) or HBSS and incubated with 1 mM IAB (Thermo Scientific) in HBSS for 3 hours at 37°C. The cells were then washed two times with PBS or HBSS and lysed by scraping them in lysis buffer [40 mM Hepes, 50 mM NaCl, 1 mM EGTA, 1 mM EDTA (pH 7.4), and 1% CHAPS] containing 1% protease inhibitor cocktail (Sigma). Insoluble material was removed by centrifugation at 14,500 rpm for 5 min. Protein concentration was determined using the Bradford assay. Biotinylated proteins were pulled down by streptavidin-coated magnetic beads (Sigma), and from this step, the same protocol was applied as for the purified protein samples, using 25 mM DTT instead of 5 mM TCEP to cleave the persulfidated proteins off the beads.

Protein persulfide detection in yeast strains by ProPerDP

To prepare protein extracts, cells in log phase were washed, resuspended in PBS + 1.2 M sorbitol, and digested with Zymolyase 100T (0.5 mg/ml; MP Biomedicals) at RT for 60 min. Yeast spheroplasts were washed and resuspended in PBS + 1.2 M sorbitol containing 5 mM of IAB and incubated at RT for 60 min. Spheroplasts were washed and resuspended in 500 μl of ice-cold lysis buffer [PBS 1×, 0.1% Triton X-100, containing protease inhibitor mix (complete, EDTA-free, Roche)]. Glass beads (Sigma) were added and cells were lysed by vigorous vortexing for 1 min at 4°C. Lysates were clarified by centrifugation at 14,000*g* at 4°C for 10 min and the ProPerDP method was then applied on the extracts.

Protein persulfide detection in frozen tissue samples by ProPerDP

Frozen tissue samples were dropped into liquid nitrogen immediately after taking them out from −80°C. A fine powder was made from these snap-frozen tissue samples in a liquid nitrogen–precooled Teflon/iridium ball Mikro Dismembrator 2 ball-mill (B. Braun Melsungen AG). IAB solution (3 mM) was added to this fine powder, and the mixture was incubated for 1 hour at RT. Following the addition of 1% CHAPS and a protease inhibitor cocktail, the mixture was incubated for an additional 30 min. Tissue debris was separated by 10-min centrifugation at 14,000*g*, and the protein content was determined in the supernatant by the Bradford method to set the protein levels to 1 mg/ml (these samples represented S1 on Fig. 1). From here, the detection method was the same as that with the A549 and HEK293 cells.

Estimation of endogenous protein persulfide levels

Protein persulfide levels in intact HEK293 cells and mouse liver tissue samples were estimated by densitometric analysis of the corresponding silver-stained gels using the ImageJ [National Institutes of Health (NIH)] or Quantity One (Bio-Rad) software. For the control cells or animal tissue samples, the optical density of the S3 fractions (representing the persulfide pool) was compared to an appropriate dilution of the cell or tissue lysates with measured total protein content ran on the same gel (n = 3 to 8 experiments). In the case of the knockdown cell lines, the relative increase in persulfide levels was calculated by comparison of the S3 samples with the corresponding control cells. Statistical significance was probed by paired t test on HEK293 cells and nonpaired t test on

tissue samples. All tests were two-sided, and a *P* value less than 0.05 was considered statistically significant.

SDS-PAGE gel electrophoresis

Samples were run on nonreducing 12% polyacrylamide gels. Equal amounts of total protein were incubated with the streptavidin-coated beads in the case of each given gel and blot, as judged by the Bradford protein assay. The total protein loadings in S1 lanes are as follows: 5 μg in Fig. 2 (A and A′), 15 μg in Fig. 2 (B and B′), 10 μg in Fig. 4A, 12 μg in Fig. 4B, 15 μg in Fig. 4D, 5 μg in fig. S1, and 10 μg in fig. S4. In the case of Fig. 2 (C and C′), S3 lanes represent the HSA persulfide fractions of 90 ng of total plasma protein. Total untreated plasma protein (100 ng) and untreated HSA (20 ng) were applied as loading controls. Similarly, only S3 lanes are shown in Fig. 5 (B and D); the corresponding S1 lanes contained 28 and 26 μg of protein, respectively (see fig. S6). Gels were visualized with colloidal Coomassie staining solution or via silver staining.

Diagonal gel electrophoresis

2D diagonal gel electrophoresis was carried out as described previously (*53*). Briefly, S1 and S2 fractions (see Fig. 1 for explanation of fractions) from A549 and HEK293 cell samples were run in 12% polyacrylamide gels, first in a nonreducing dimension and then in a reducing dimension and the obtained gels were silver-stained. The spots located in the upper half of the gels (above the diagonal) correspond to proteins containing intramolecular disulfide bonds, whereas proteins intermolecularly linked by disulfide bonds are found below the diagonal.

Western blotting against HSA

Following SDS-PAGE gel electrophoresis, plasma samples were transferred to polyvinylidene difluoride membranes and blocked overnight in 3% BSA solution at 4°C. Membranes were then incubated for 1 hour in anti-albumin antibody (Sigma A0433), diluted 1:10,000 in 3% BSA. Subsequently, the membranes were washed three times with TBST buffer and incubated for 1 hour in alkaline phosphatase–conjugated secondary antibody (Sigma A3687), diluted 1:10,000 in 3% BSA. Membranes were washed again three times in TBST buffer, and the bands were visualized by 5-bromo-4-chloro-3-indolyl phosphate–nitro blue tetrazolium (Merck).

Enzyme kinetic studies

All kinetic experiments were carried out in TE buffer (50 mM tris-HCl and 2 mM EDTA, pH 7.5) at RT, in 96-well microtiter plates. NADPH consumption was followed at 340 nm, the absorption maximum of reduced NADPH. In a typical kinetic experiment, the calculated amount of polysulfide or persulfide sample was pipetted in the plate and the assay was started by the addition of a Master Mixture, containing the appropriate amount of NADPH, TrxR1, Trx1, or TPR14, or alternatively, NADPH, GSH, GR, and Grx1 as indicated. Initial rates from each run were calculated from the slopes of the linear ranges of the curves. Turnover was calculated using an NADPH standard curve and dividing the initial rate with the concentration of TrxR1 (Fig. 3).

A549 cell cultures

The A549 human lung carcinoma cell line was obtained from the European Collection of Cell Cultures (ECACC 12H017) (Sigma) and cultured in DMEM (Dulbecco's modified Eagle's medium)–F12 medium (Lonza) supplemented with 10% (v/v) heat-inactivated fetal bovine serum (FBS), penicillin (100 U/ml), and streptomycin (100 μg/ml) (Sigma) at 37°C in a humidified atmosphere of 5% CO_2. A549 cells were free of mycoplasma contamination tested by the MycoSensor QPCR Assay Kit (Agilent Technologies).

Generation of stably transfected HEK293 cells

HEK293 cells were from the American Type Culture Collection (ATCC) and were cultured in Eagle's minimum essential medium (ATCC), complemented with 10% (v/v) FBS (PAA Laboratories), penicillin, (100 U/ml), and streptomycin (100 μg/ml) (Biochrom AG). Cells were kept in logarithmic growth phase at 37°C in humidified air containing 5% CO_2. Knockdown of TRP14 and TrxR1 was performed using shRNA-bearing plasmids [from Qiagen, KH19389H (human TXNDC17, encoding TRP14) and KH02104H (human TXNRD1)] for the respective proteins as described earlier (*22*). A negative control shRNA plasmid was included as a control. For stable knockdown, HEK293 cells were seeded in six-well plates at a density of 4×10^5 cells per well 24 hours before transfection. All plasmids were transfected using TurboFect (Thermo Scientific) as transfection reagent with 0.6 μg DNA and 1.2 μl TurboFect per well. Transfected cells were selected by adding Hygromycin B (0.1 mg/ml; Invitrogen) to the growth medium 72 hours after transfection. After approximately 3 weeks, separate populations of stably transfected cells were generated by selecting single resistant cell clones. Selection was continued until enough cells were available for generation of freezing stocks. The knockdown was verified in all clones by Western blot using antibodies against TrxR1 (sc-58444) and TRP14 (R&D Systems MAB3504), and GAPDH was used as a loading control (sc-25778). Upon validation, Hygromycin B was removed from the growth medium, which did not affect the knockdown of the proteins over several passages. HEK293 cells were free of mycoplasma contamination tested by the MycoSensor QPCR Assay Kit (Agilent Technologies).

Yeast strains

Yeast strains used in this work were derived from BY4742 (*54*) and are described in Table 1. *Saccharomyces cerevisiae* cells were grown at 30°C in Synthetic Complete medium (6.7 g of yeast nitrogen bases without amino acids, 1.89 g/liter of drop-out mix containing all the amino acids and supplements, and 20 g/liter of dextrose).

Sulforhodamine B assay for cytotoxicity screening

Sulforhodamine B (SRB) assay was performed as described by Vichai *et al.* (*55*). HEK293 (control and TrxR1 knockdown) cells (5×10^3) were seeded to 96-well cell culture plates per well and incubated for 24 hours at 37°C in 5% CO_2 atmosphere. After 24 hours, 0.2 to 3 mM HS_x^- was added in HBSS and cells were incubated for 2 hours. After the exposure period with polysulfide, HBSS was replaced by complete cell growth medium and SRB assay was performed after 24 hours. Before fixation, cells were rinsed with HBSS. Cells were fixed by adding 100 μl of 10% ice-cold trichloroacetic acid to each well, incubated at 4°C for 1 hour, and then washed with distilled water. Fifty microliters of SRB stain (0.4%

Table 1. Yeast strains used in the present study.

Strain	Relevant genotype	Source
BY4742 (WT)	*MATα his3Δ1 leu2Δ lys2Δ ura3Δ*	(*54*)
cys3Δ (CSE deleted)	BY4742 cys3::KanMX4	(*59*)
cys4Δ (CBS deleted)	BY4742 cys4::KanMX4	(*59*)

in 1% acetic acid) was added to each well and incubated for 15 min at RT. The plates were rinsed four times with 1% acetic acid and 200 µl of 10 mM tris base solution (pH 10.5) was added to each well, and the plates were shaken for 5 min to solubilize the protein-bound dye. Absorbance was read on a plate reader (BioTek) at 570 nm. Cell survival was measured as absorbance (optical density) of the mean of the 12 replicate wells compared to the control (no polysulfide-treated wells). Paired *t* test was performed using the GraphPad Prism Software.

There was a slight difference in the proliferation of the untreated wild-type and TrxR1 knockout cells after 24 hours. Control cells had about 12% higher proliferation rate; however, this was statistically not significant (*t* test, $P = 0.14$). Nonetheless, to correct for this difference, results obtained from the SRB assay are presented as

$$\%\ \text{of control cell growth} = \frac{\text{mean OD sample 24 hours} - \text{mean OD sample 2 hours}}{\text{mean OD neg control 24 hours} - \text{mean OD neg control 2 hours}} \times 100$$

Hence, in all cases, dose-response data upon polysulfide treatment were corrected with the untreated control cell growth, so that differences to untreated cell proliferation were taken into account.

Mass spectrometry analysis

After destaining of QC Colloidal Coomassie Blue (Bio-Rad)–stained SDS-PAGE gels with H_2O:CH_3OH:CH_3COOH (5:4:1), the indicated bands were cut out, reduced with DTT, alkylated with iodoacetamide, and then digested with trypsin from porcine pancreas (dimethylated, proteomics grade, Sigma) as suggested by the UCSF (University of California, San Francisco) Mass Spectrometry Core Facility (*56*, *57*). Before liquid chromatography–mass spectrometry measurements, the digested samples were cleaned with C18 ZipTip pipette tips (Millipore). Tryptic peptides were separated by reversed-phase chromatography with a nanoflow high-performance liquid chromatography (HPLC) (Easy nLC II, Thermo Fisher Scientific) system on an EASY-column (10 cm, 75 µm, C18) using gradient elution [developed from 5% (v/v) acetonitrile, 0.1% (v/v) formic acid to 90% (v/v) acetonitrile, 0.1% (v/v) formic acid in water over 40 min at a flow rate of 300 nl/min]. The nanoflow HPLC system was coupled to an LTQ XL ion trap mass spectrometer (Thermo Fisher Scientific) for peptide analyses that was conducted in triple play positive ion mode in a mass range between 400 and 1500 *m*/*z* (mass/charge ratio). All tandem mass spectrometry samples were analyzed using ProteinProspector (UCSF Mass Spectrometry Facility, v 5.14.1). Data were searched against NCBI (National Center for Biotechnology Information) no. 2013.06.17 database with *Homo sapiens* as taxonomy. One missed cleavage was allowed.

Preparation of mouse liver tissue samples

Mouse care and use were performed at Montana State University (MSU) following guidelines set forth by the U.S. NIH and outlined in the current *Guide for the Care and Use of Laboratory Animals* (*58*). Animal protocols were approved by the MSU Institutional Animal Care and Use Committee. The alleles, allelic combinations, and detailed care conditions have been described previously (*34*). Eight- to 10-week-old males of the indicated genotypes were euthanized, and livers were perfused by a cardiac-to-portal route with a solution of 150 mM NaCl, 100 mM Pipes (pH 7.1), and 3.0 mM IAB. Perfused livers were removed and divided into ~100-mg pieces, and each was submerged in a 1.5-ml tube containing perfusion buffer. Samples were incubated on ice for 15 to 20 min, excess perfusion buffer was removed, tubes were sealed, and the samples were snap-frozen in liquid nitrogen. Samples were kept at −80°C or on dry ice until use.

SUPPLEMENTARY MATERIALS

Supplementary material for this article is available at http://advances.sciencemag.org/cgi/content/full/2/1/e1500968/DC1

Fig. S1. HSA persulfide is reduced to HSA by sulfide in a dose-dependent manner.
Fig. S2. Selenite-reducing TrxR1 activity is not inhibited by polysulfides.
Fig. S3. Compromised polysulfide reduction by TrxR1 mutants lacking the Sec residue.
Fig. S4. Detection of persulfide formation on BSA.
Fig. S5. BSA-SSH reduction by NADPH/TrxR1-coupled Trx1 and TRP14.
Fig. S6. Relative efficiency of alkylation and streptavidin pulldown in the ProPerDP method applied to control and TrxR1 or TRP14 knockdown HEK293 cells.
Fig. S7. Control experiment to the BSA-SSH reduction by the NADPH/GR/GSH-coupled Grx1 experiment (see Fig. 6 in the main text).
Fig. S8. Endogenously detected protein persulfides exhibit elevated levels in HS_x^--treated TrxR1, TRP14 knockdown, or control HEK293 cells.
Fig. S9. Diagonal gel electrophoresis experiment corroborates that false-positive hits outlined in Fig. 8B by ProPerDP are of minor importance.
Fig. S10. Suggested scheme for polysulfide reduction by the NADPH/TrxR1-coupled TRP14 system.

REFERENCES AND NOTES

1. K. Abe, H. Kimura, The possible role of hydrogen sulfide as an endogenous neuromodulator. *J. Neurosci.* **16**, 1066–1071 (1996).
2. R. Wang, Physiological implications of hydrogen sulfide: A whiff exploration that blossomed. *Physiol. Rev.* **92**, 791–896 (2012).
3. C. Szabo, Gaseotransmitters: New frontiers for translational science. *Sci. Transl. Med.* **2**, 59ps54 (2010).
4. J. L. Wallace, R. Wang, Hydrogen sulfide-based therapeutics: Exploiting a unique but ubiquitous gasotransmitter. *Nat. Rev. Drug Discov.* **14**, 329–345 (2015).
5. P. Nagy, Chapter one—Mechanistic chemical perspective of hydrogen sulfide signaling. *Methods Enzymol.* **554**, 3–29 (2015).
6. B. D. Paul, S. H. Snyder, H_2S signalling through protein sulfhydration and beyond. *Nat. Rev. Mol. Cell Biol.* **13**, 499–507 (2012).
7. T. Ida, T. Sawa, H. Ihara, Y. Tsuchiya, Y. Watanabe, Y. Kumagai, M. Suematsu, H. Motohashi, S. Fujii, T. Matsunaga, M. Yamamoto, K. Ono, N. O. Devarie-Baez, M. Xian, J. M. Fukuto, T. Akaike, Reactive cysteine persulfides and S-polythiolation regulate oxidative stress and redox signaling. *Proc. Natl. Acad. Sci. U.S.A.* **111**, 7606–7611 (2014).
8. O. Kabil, R. Banerjee, Redox biochemistry of hydrogen sulfide. *J. Biol. Chem.* **285**, 21903–21907 (2010).
9. C. Coletta, A. Papapetropoulos, K. Erdelyi, G. Olah, K. Módis, P. Panopoulos, A. Asimakopoulou, D. Gerö, I. Sharina, E. Martin, C. Szabo, Hydrogen sulfide and nitric oxide are mutually dependent in the regulation of angiogenesis and endothelium-dependent vasorelaxation. *Proc. Natl. Acad. Sci. U.S.A.* **109**, 9161–9166 (2012).
10. M. M. Cortese-Krott, B. O. Fernandez, J. L. T. Santos, E. Mergia, M. Grman, P. Nagy, M. Kelm, A. Butler, M. Feelisch, Nitrosopersulfide ($SSNO^-$) accounts for sustained NO bioactivity of S-nitrosothiols following reaction with sulfide. *Redox Biol.* **2**, 234–244 (2014).
11. M. M. Cortese-Krott, G. G. C. Kuhnle, A. Dyson, B. O. Fernandez, M. Grman, J. F. DuMond, M. P. Barrow, G. McLeod, H. Nakagawa, K. Ondrias, P. Nagy, S. B. King, J. E. Saavedra, L. K. Keefer, M. Singer, M. Kelm, A. R. Butler, M. Feelisch, The key bioactive reaction products of the NO/H_2S interaction are S/N-hybrid species, polysulfides, and nitroxyl. *Proc. Natl. Acad. Sci. U.S.A.* **112**, E4651–E4660 (2015).
12. G. K. Kolluru, X. Shen, C. G. Kevil, A tale of two gases: NO and H_2S, foes or friends for life? *Redox Biol.* **1**, 313–318 (2013).
13. H. Kimura, Signaling molecules: Hydrogen sulfide and polysulfide. *Antioxid. Redox Signal.* **22**, 362–376 (2015).
14. K. Ono, T. Akaike, T. Sawa, Y. Kumagai, D. A. Wink, D. J. Tantillo, A. J. Hobbs, P. Nagy, M. Xian, J. Lin, J. M. Fukuto, Redox chemistry and chemical biology of H_2S, hydropersulfides, and derived species: Implications of their possible biological activity and utility. *Free Radic. Biol. Med.* **77**, 82–94 (2014).
15. V. S. Lin, W. Chen, M. Xian, C. J. Chang, Chemical probes for molecular imaging and detection of hydrogen sulfide and reactive sulfur species in biological systems. *Chem. Soc. Rev.* **44**, 4596–4618 (2014).

16. C.-M. Park, I. Macinkovic, M. R. Filipovic, M. Xian, Chapter three—Use of the "tag-switch" method for the detection of protein S-sulfhydration. *Methods Enzymol.* **555**, 39–56 (2015).
17. J. I. Toohey, Sulfur signaling: Is the agent sulfide or sulfane? *Anal. Biochem.* **413**, 1–7 (2011).
18. T. V. Mishanina, M. Libiad, R. Banerjee, Biogenesis of reactive sulfur species for signaling by hydrogen sulfide oxidation pathways. *Nat. Chem. Biol.* **11**, 457–464 (2015).
19. Y. Mikami, N. Shibuya, Y. Kimura, N. Nagahara, Y. Ogasawara, H. Kimura, Thioredoxin and dihydrolipoic acid are required for 3-mercaptopyruvate sulfurtransferase to produce hydrogen sulfide. *Biochem. J.* **439**, 479–485 (2011).
20. N. Krishnan, C. Fu, D. J. Pappin, N. K. Tonks, H_2S-induced sulfhydration of the phosphatase PTP1B and its role in the endoplasmic reticulum stress response. *Sci. Signal.* **4**, ra86 (2011).
21. W. Jeong, H. W. Yoon, S.-R. Lee, S. G. Rhee, Identification and characterization of TRP14, a thioredoxin-related protein of 14 kDa. New insights into the specificity of thioredoxin function. *J. Biol. Chem.* **279**, 3142–3150 (2004).
22. I. Pader, R. Sengupta, M. Cebula, J. Xu, J. O. Lundberg, A. Holmgren, K. Johansson, E. S. J. Arnér, Thioredoxin-related protein of 14 kDa is an efficient L-cystine reductase and S-denitrosylase. *Proc. Natl. Acad. Sci. U.S.A.* **111**, 6964–6969 (2014).
23. R. Greiner, Z. Pálinkás, K. Bäsell, D. Becher, H. Antelmann, P. Nagy, T. P. Dick, Polysulfides link H_2S to protein thiol oxidation. *Antioxid. Redox Signal.* **19**, 1749–1765 (2013).
24. P. Nagy, Z. Pálinkás, A. Nagy, B. Budai, I. Tóth, A. Vasas, Chemical aspects of hydrogen sulfide measurements in physiological samples. *Biochim. Biophys. Acta* **1840**, 876–891 (2014).
25. A. Vasas, É. Dóka, I. Fábián, P. Nagy, Kinetic and thermodynamic studies on the disulfide-bond reducing potential of hydrogen sulfide. *Nitric Oxide* **46**, 93–101 (2015).
26. E. A. Wintner, T. L. Deckwerth, W. Langston, A. Bengtsson, D. Leviten, P. Hill, M. A. Insko, R. Dumpit, E. VandenEkart, C. F. Toombs, C. Szabo, A monobromobimane-based assay to measure the pharmacokinetic profile of reactive sulphide species in blood. *Br. J. Pharmacol.* **160**, 941–957 (2010).
27. X. Shen, E. A. Peter, S. Bir, R. Wang, C. G. Kevil, Analytical measurement of discrete hydrogen sulfide pools in biological specimens. *Free Radic. Biol. Med.* **52**, 2276–2283 (2012).
28. E. S. J. Arnér, Focus on mammalian thioredoxin reductases—Important selenoproteins with versatile functions. *Biochim. Biophys. Acta* **1790**, 495–526 (2009).
29. Q. Cheng, T. Sandalova, Y. Lindqvist, E. S. J. Arnér, Crystal structure and catalysis of the selenoprotein thioredoxin reductase 1. *J. Biol. Chem.* **284**, 3998–4008 (2009).
30. S. Kumar, M. Björnstedt, A. Holmgren, Selenite is a substrate for calf thymus thioredoxin reductase and thioredoxin and elicits a large non-stoichiometric oxidation of NADPH in the presence of oxygen. *Eur. J. Biochem.* **207**, 435–439 (1992).
31. A. K. Mustafa, M. M. Gadalla, N. Sen, S. Kim, W. Mu, S. K. Gazi, R. K. Barrow, G. Yang, R. Wang, S. H. Snyder, H_2S signals through protein S-sulfhydration. *Sci. Signal.* **2**, ra72 (2009).
32. O. Kabil, R. Banerjee, Enzymology of H_2S biogenesis, decay and signaling. *Antioxid. Redox Signal.* **20**, 770–782 (2014).
33. C. H. Lillig, C. Berndt, A. Holmgren, Glutaredoxin systems. *Biochim. Biophys. Acta* **1780**, 1304–1317 (2008).
34. S. Eriksson, J. R. Prigge, E. A. Talago, E. S. J. Arnér, E. E. Schmidt, Dietary methionine can sustain cytosolic redox homeostasis in the mouse liver. *Nat. Commun.* **6**, 6479 (2015).
35. N. Sen, B. D. Paul, M. M. Gadalla, A. K. Mustafa, T. Sen, R. Xu, S. Kim, S. H. Snyder, Hydrogen sulfide-linked sulfhydration of NF-κB mediates its antiapoptotic actions. *Mol. Cell* **45**, 13–24 (2012).
36. K. Zhao, Y. Ju, S. Li, Z. Altaany, R. Wang, G. Yang, S-sulfhydration of MEK1 leads to PARP-1 activation and DNA damage repair. *EMBO Rep.* **15**, 792–800 (2014).
37. A. K. Mustafa, G. Sikka, S. K. Gazi, J. Steppan, S. M. Jung, A. K. Bhunia, V. M. Barodka, F. K. Gazi, R. K. Barrow, R. Wang, L. M. Amzel, D. E. Berkowitz, S. H. Snyder, Hydrogen sulfide as endothelium-derived hyperpolarizing factor sulfhydrates potassium channels. *Circ. Res.* **109**, 1259–1268 (2011).
38. D. Zhang, I. Macinkovic, N. O. Devarie-Baez, J. Pan, C.-M. Park, K. S. Carroll, M. R. Filipovic, M. Xian, Detection of protein S-sulfhydration by a tag-switch technique. *Angew. Chem. Int. Ed. Engl.* **53**, 575–581 (2014).
39. J. Pan, K. S. Carroll, Persulfide reactivity in the detection of protein S-sulfhydration. *ACS Chem. Biol.* **8**, 1110–1116 (2013).
40. P. Nagy, Kinetics and mechanisms of thiol–disulfide exchange covering direct substitution and thiol oxidation-mediated pathways. *Antioxid. Redox Signal.* **18**, 1623–1641 (2013).
41. Y.-M. Go, J. D. Chandler, D. P. Jones, The cysteine proteome. *Free Radic. Biol. Med.* **84**, 227–245 (2015).
42. R. E. Hansen, D. Roth, J. R. Winther, Quantifying the global cellular thiol–disulfide status. *Proc. Natl. Acad. Sci. U.S.A.* **106**, 422–427 (2009).
43. A. Miseta, P. Csutora, Relationship between the occurrence of cysteine in proteins and the complexity of organisms. *Mol. Biol. Evol.* **17**, 1232–1239 (2000).
44. M. Dagnell, J. Frijhoff, I. Pader, M. Augsten, B. Boivin, J. Xu, P. K. Mandal, N. K. Tonks, C. Hellberg, M. Conrad, E. S. J. Arnér, A. Östman, Selective activation of oxidized PTP1B by the thioredoxin system modulates PDGF-β receptor tyrosine kinase signaling. *Proc. Natl. Acad. Sci. U.S.A.* **110**, 13398–13403 (2013).
45. J. Lu, A. Holmgren, The thioredoxin antioxidant system. *Free Radic. Biol. Med.* **66**, 75–87 (2014).
46. F. Zahedi Avval, A. Holmgren, Molecular mechanisms of thioredoxin and glutaredoxin as hydrogen donors for Mammalian s phase ribonucleotide reductase. *J. Biol. Chem.* **284**, 8233–8240 (2009).
47. P. Nagy, C. C. Winterbourn, Rapid reaction of hydrogen sulfide with the neutrophil oxidant hypochlorous acid to generate polysulfides. *Chem. Res. Toxicol.* **23**, 1541–1543 (2010).
48. E. S. J. Arnér, H. Sarioglu, F. Lottspeich, A. Holmgren, A. Böck, High-level expression in *Escherichia coli* of selenocysteine-containing rat thioredoxin reductase utilizing gene fusions with engineered bacterial-type SECIS elements and co-expression with the *selA*, *selB* and *selC* genes. *J. Mol. Biol.* **292**, 1003–1016 (1999).
49. J. Xu, S. E. Eriksson, M. Cebula, T. Sandalova, E. Hedström, I. Pader, Q. Cheng, C. R. Myers, W. E. Antholine, P. Nagy, U. Hellman, G. Selivanova, Y. Lindqvist, E. S. J. Arnér, The conserved Trp114 residue of thioredoxin reductase 1 has a redox sensor-like function triggering oligomerization and crosslinking upon oxidative stress related to cell death. *Cell Death Dis.* **6**, e1616 (2015).
50. Q. Cheng, S. Stone-Elander, E. S. J. Arnér, Tagging recombinant proteins with a Sel-tag for purification, labeling with electrophilic compounds or radiolabeling with ^{11}C. *Nat. Protoc.* **1**, 604–613 (2006).
51. O. Rengby, L. Johansson, L. A. Carlson, E. Serini, A. Vlamis-Gardikas, P. Kårsnäs, E. S. J. Arnér, Assessment of production conditions for efficient use of *Escherichia coli* in high-yield heterologous recombinant selenoprotein synthesis. *Appl. Environ. Microbiol.* **70**, 5159–5167 (2004).
52. J. E. Tropea, S. Cherry, D. S. Waugh, Expression and purification of soluble His_6-tagged TEV protease. *Methods Mol. Biol.* **498**, 297–307 (2009).
53. B. McDonagh, Diagonal electrophoresis for detection of protein disulphide bridges. *Methods Mol. Biol.* **519**, 305–310 (2009).
54. C. B. Brachmann, A. Davies, G. J. Cost, E. Caputo, J. Li, P. Hieter, J. D. Boeke, Designer deletion strains derived from *Saccharomyces cerevisiae* S288C: A useful set of strains and plasmids for PCR-mediated gene disruption and other applications. *Yeast* **14**, 115–132 (1998).
55. V. Vichai, K. Kirtikara, Sulforhodamine B colorimetric assay for cytotoxicity screening. *Nat. Protoc.* **1**, 1112–1116 (2006).
56. A. Shevchenko, M. Wilm, O. Vorm, M. Mann, Mass spectrometric sequencing of proteins from silver-stained polyacrylamide gels. *Anal. Chem.* **68**, 850–858 (1996).
57. J. Havliš, H. Thomas, M. Šebela, A. Shevchenko, Fast-response proteomics by accelerated in-gel digestion of proteins. *Anal. Chem.* **75**, 1300–1306 (2003).
58. J. C. Garber, R. W. Barbee, J. T. Bielitzki, L. A. Clayton, J. C. Donovan, D. F. Kohn, N. S. Lipman, P. Locke, J. Melcher, F. W. Quimby, P. V. Turner, G. A. Wood, H. Wurbel, *Guide for the Care and Use of Laboratory Animals* (The National Academies Press, Washington DC, ed. 8, 2011).
59. E. A. Winzeler, D. D. Shoemaker, A. Astromoff, H. Liang, K. Anderson, B. Andre, R. Bangham, R. Benito, J. D. Boeke, H. Bussey, A. M. Chu, C. Connelly, K. Davis, F. Dietrich, S. W. Dow, M. El Bakkoury, F. Foury, S. H. Friend, E. Gentalen, G. Giaever, J. H. Hegemann, T. Jones, M. Laub, H. Liao, N. Liebundguth, D. J. Lockhart, A. Lucau-Danila, M. Lussier, N. M'Rabet, P. Menard, M. Mittmann, C. Pai, C. Rebischung, J. L. Revuelta, L. Riles, C. J. Roberts, P. Ross-MacDonald, B. Scherens, M. Snyder, S. Sookhai-Mahadeo, R. K. Storms, S. Véronneau, M. Voet, G. Volckaert, T. R. Ward, R. Wysocki, G. S. Yen, K. Yu, K. Zimmermann, P. Philippsen, M. Johnston, R. W. Davis, Functional characterization of the *S. cerevisiae* genome by gene deletion and parallel analysis. *Science* **285**, 901–906 (1999).

Acknowledgments: Z. Pálinkás is acknowledged for his help in mass spectrometric analyses, C. Miller and I. Cavigli are acknowledged for their assistance in liver harvests, and B. Budai is acknowledged for his advice in statistical analyses. Human Grx1 was provided by A. Holmgren. **Funding:** Financial support from FP7-PEOPLE-2010-RG (Marie Curie International Reintegration grant no. PIRG08-GA-2010-277006) and The Hungarian National Science Foundation (grant no. K 109843) to P.N. and from the Swedish Research Council, the Swedish Cancer Society, and Karolinska Institutet to E.S.J.A is acknowledged. P.N. is a János Bolyai Research Scholar of the Hungarian Academy of Sciences. É.D. is grateful for COST action BM1005 for an STSM grant support to carry out most of the TrxR1, Trx1, and TRP14 experiments in E.S.J.A.'s laboratory. E.E.S. was supported by grants AG040020 and GM110732 from the U.S. NIH and by an award from the Swedish Wenner-Gren Foundation. T.P.D. acknowledges support from the German Research Foundation (SFB 1036 and SPP 1710). **Author contributions:** É.D. was responsible for most of the experimental work, and she was involved in data analyses and contributed to writing the paper. I.P. conducted and assisted with the kinetic experiments, expressed and purified TRP14 protein, and constructed the TrxR1 and TRP14 knockdown cell lines. A.B. conducted cell biology experiments and the initial assays with HSA. K.J. assisted with the generation of the knockdown cell lines. Q.C. expressed and purified TrxR1 and Trx1 proteins. K.B. assisted with the cellular experimentations. D.P.-F. carried out experimental work with yeast. T.P.D. designed experiments and provided essential intellectual input. J.R.P. and E.E.S. prepared and provided mouse liver tissue samples, and E.E.S. provided essential intellectual input. E.S.J.A designed experiments, analyzed data, provided essential intellectual input, and contributed to writing the paper. P.N. conceived the study and had overall responsibility for the project; he contributed to the design and interpretation of experimental results and wrote the paper. **Competing interests:** The authors declare that they have no competing interests. **Data and materials availability:** All data needed to evaluate the conclusions in the paper are present in the paper and/or the Supplementary Materials. Additional data related to this paper are available from the authors upon request at peter.nagy@oncol.hu.

Submitted 20 July 2015
Accepted 20 November 2015
Published 22 January 2016
10.1126/sciadv.1500968

Citation: É. Dóka, I. Pader, A. Bíró, K. Johansson, Q. Cheng, K. Ballagó, J. R. Prigge, D. Pastor-Flores, T. P. Dick, E. E. Schmidt, E. S. J. Arnér, P. Nagy, A novel persulfide detection method reveals protein persulfide- and polysulfide-reducing functions of thioredoxin and glutathione systems. *Sci. Adv.* **2**, e1500968 (2016).

ScienceAdvances
AAAS

A novel persulfide detection method reveals protein persulfide- and polysulfide-reducing functions of thioredoxin and glutathione systems

Éva Dóka, Irina Pader, Adrienn Bíró, Katarina Johansson, Qing Cheng, Krisztina Ballagó, Justin R. Prigge, Daniel Pastor-Flores, Tobias P. Dick, Edward E. Schmidt, Elias S. J. Arnér and Péter Nagy (January 22, 2016)
Sci Adv 2016, 2:.
doi: 10.1126/sciadv.1500968